



MODELING AND SIMULATION ARCHITECTURE
FOR STUDYING DOPPLER-BASED RADAR
WITH COMPLEX ENVIRONMENTS

THESIS

Nicholas J. Amato, Captain, USAF

AFIT/GE/ENG/09-02

DEPARTMENT OF THE AIR FORCE
AIR UNIVERSITY

AIR FORCE INSTITUTE OF TECHNOLOGY

Wright-Patterson Air Force Base, Ohio

APPROVED FOR PUBLIC RELEASE; DISTRIBUTION UNLIMITED.

The views expressed in this thesis are those of the author and do not reflect the official policy or position of the United States Air Force, Department of Defense, or the United States Government.

AFIT/GE/ENG/09-02

MODELING AND SIMULATION ARCHITECTURE
FOR STUDYING DOPPLER-BASED RADAR
WITH COMPLEX ENVIRONMENTS

THESIS

Presented to the Faculty
Department of Electrical and Computer Engineering
Graduate School of Engineering and Management
Air Force Institute of Technology
Air University
Air Education and Training Command
In Partial Fulfillment of the Requirements for the
Degree of Master of Science in Electrical Engineering

Nicholas J. Amato, B.S.E.E.
Captain, USAF

March 2009

APPROVED FOR PUBLIC RELEASE; DISTRIBUTION UNLIMITED.

MODELING AND SIMULATION ARCHITECTURE
FOR STUDYING DOPPLER-BASED RADAR
WITH COMPLEX ENVIRONMENTS

Nicholas J. Amato, B.S.E.E.
Captain, USAF

Approved:

/signed/

19 Mar 2009

Maj M.A. Saville, PhD (Chairman)

date

/signed/

19 Mar 2009

Maj M.J. Mendenhall, PhD (Member)

date

/signed/

19 Mar 2009

Dr. M.C. Fickus, PhD (Member)

date

Abstract

This research effort develops a hybrid large-scale modeling and simulation framework that defines the requirements for a program to evaluate radar-aircraft-turbine-clutter interactions. Wind turbines and other moving structures can interfere with a radar's ability to detect moving aircraft because radar returns from turbines are comparable to those from slow flying aircraft. This interference can lead to aircraft collisions or crashes, reducing the safety for air traffic.

Two radar applications, *INSSITE* and *IMOM*, were investigated to determine which of the subsystems, in the proposed architecture, are currently available and which need additional development. Current radar applications either delve too deep into details, requiring years to process, or too shallow, ignoring the Doppler effect and assuming a static scattering value. Engineering-level radar, radiation, propagation, and scattering models are already developed. However, engagement-level stochastic scattering, amplitude and phase, data aren't available. The hybrid modeling and simulation architecture could be realized once stochastic RCS models are developed.

Acknowledgements

I'd like to thank everyone that helped me in many ways great and small.

I'd like to specifically thank several people. Maj. Saville for his guidance and encouragement. Maj. Mendenhall and Dr. Temple for the hardware necessary for this research. Capt. Brand for his support and for being my goto guy for everything ARSR-4 related. Lt. Hemperly and Mr. Peltier for their assistance getting *IMOM* up and running. Mr. Gloekler, Mr. Shargo, and Mr. Lindquist for their help on operating *INSSITE*. Most importantly, thank you to my family and friends for all your support, encouragement, and putting up with me.

Nicholas J. Amato

Table of Contents

	Page
Abstract	iv
Acknowledgements	v
Table of Contents	vi
List of Figures	ix
List of Tables	xi
List of Abbreviations	xii
I. Introduction	1
1.1 Background	1
1.2 Problem Statement	1
1.3 Proposed Solution	3
1.4 Sponsors	3
1.4.1 84 RADES	3
1.4.2 NASIC	3
1.4.3 453rd EWS	3
II. Literature Review	5
2.1 Radar Basics	5
2.1.1 Radar Range Equation	5
2.1.2 Primary vs Secondary Surveillance Radar	5
2.2 Wind Turbine Physics	6
2.2.1 Line of Sight	6
2.2.2 Radar Cross-Section	7
2.2.3 Doppler Effect	9
2.3 Wind Turbine Effects on Radar	12
2.3.1 Shadow Zone	13
2.3.2 Clutter	14
2.3.3 Raised Threshold	15
2.3.4 False Moving Targets	15
2.3.5 Tracking	19
2.3.6 Receiver Saturation	19
2.4 Modeling Wind Turbine RCS	20
2.5 Large Scale Modeling and Simulation	21
2.5.1 How Large is Large?	21

	Page	
2.5.2	Who Uses Large-Scale M&S?	22
2.5.3	M&S Hierarchy	22
III.	Methodology	25
3.1	Overview	25
3.2	Evaluating Complexity	26
3.2.1	Physics-Level	26
3.2.2	Engineering-Level	27
3.2.3	Engagement-Level	27
3.3	Architecture Development	28
3.4	Existing Programs	28
3.5	Experimental Simulations	29
3.5.1	<i>IMOM</i> Experiments	29
3.5.2	<i>INSSITE</i> Experiments	30
3.5.3	Underlying Mathematics	31
3.6	Analyzing the Architecture	33
IV.	Radar-based Modeling and Simulation	34
4.1	Connection Diagrams	34
4.1.1	Mission-Level	34
4.1.2	Engagement-Level	36
4.1.3	Engineering-Level	37
4.1.4	Physics-Level	39
4.2	Features	39
4.2.1	Display	40
4.2.2	Radar	40
4.2.3	Target	42
4.2.4	EM - Propagation	43
4.3	Understanding Computational Requirements	44
4.4	Rationale behind Tip Speed - Wind States	46
V.	<i>IMOM</i> and <i>INSSITE</i> Experiments	48
5.1	<i>IMOM</i>	48
5.1.1	Overview	48
5.1.2	Experimental Results	48
5.1.3	Mission-Level	52
5.1.4	Engagement-Level	52
5.1.5	Engineering-Level	52
5.1.6	Physics-Level	53
5.1.7	Limitations	53

	Page
5.2 INNSITE	53
5.2.1 Overview	53
5.2.2 Experimental Results	54
5.2.3 Mission-Level	57
5.2.4 Engagement-Level	57
5.2.5 Engineering-Level	57
5.2.6 Physics-Level	57
5.2.7 Limitations	57
VI. Conclusions	59
6.1 Conclusions	59
6.2 Additional Research	60
Bibliography	61

List of Figures

Figure		Page
1.1.	Typical Wind Turbine	2
2.1.	2-D Radar Coverage Slice	7
2.2.	Measured vs Simulated RCS	8
2.3.	Turbine Power vs Wind Speed	10
2.4.	Tip Speed vs Wind Speed	11
2.5.	Turbine Doppler	11
2.6.	Impact of Angle on Doppler	12
2.7.	Terrain Masking Shadow Zones	15
2.8.	Clutter vs Resolution Cells	16
2.9.	Clutter Maps	16
2.10.	Turbine Blades and Aircraft	18
2.11.	Maximum Doppler vs Angle - Wind States	21
2.12.	RCS Magnitude Calculation	22
2.13.	Modeling and Simulation Pyramid	23
2.14.	Army Military Planning Spectrum	24
3.1.	Development Flowchart	25
3.2.	RCS Complexity	26
3.3.	Statistical RCS	27
3.4.	Range Ring	32
4.1.	Mission-Level Simulation	35
4.2.	FAA - OE/AAA Map	36
4.3.	Engagement-Level Simulation	37
4.4.	Radar Engineering-Level Model	38
4.5.	Physics-Level EM Wave Scattering	39
4.6.	ARSR-4 Processor	42

Figure		Page
4.7.	Discrete set of turbine positions	43
4.8.	LOS Analysis Tool	44
4.9.	Three Propagation Models	45
4.10.	Physics-Level EM Wave Scattering	47
5.1.	IMOM LOS	49
5.2.	IMOM Aircraft Detection	50
5.3.	IMOM Turbine Detection	50
5.4.	Simulated Turbine - DTED Level 2	51
5.5.	Simulated Turbine - DTED Level 1	52
5.6.	INSSITE - Terrain	54
5.7.	INSSITE - Turbine Convergence	55
5.8.	INSSITE - Turbine + Terrain	55
5.9.	INSSITE - Aircraft + Terrain	56
5.10.	INSSITE - Aircraft + Turbine + Terrain	56

List of Tables

Table		Page
2.1.	Order of significance for PSR impacts, 1 is highest [13]	13
2.2.	L-Band rule-of-thumb Shadow Length	14
2.3.	L-Band (1 GHz) rule-of-thumb RCS values [14]	17
2.4.	Proposed Wind States [8].	20
4.1.	Sample radar and turbine parameters	44

List of Abbreviations

Abbreviation		Page
AD	Air Defense	1
ATC	Air Traffic Control	1
DoD	Department of Defense	1
RCS	Radar Cross Section	2
RADES	Radar Evaluation Squadron	3
NASIC	National Air and Space Intelligence Center	3
<i>INSSITE</i>	Interactive Sensor Simulator for Terrain Environments	3
EWS	Electronic Warfare Squadron	3
IO	Information Operations	3
DTED	Digital Terrain Elevation Data	4
<i>IMOM</i>	Improved Many-On-Many	4
PSR	Primary Surveillance Radar	5
SSR	Secondary Surveillance Radar	6
LOS	Line-of-Sight	6
CEM	Computational Electromagnetic	7
AFRL	Air Force Research Laboratory	8
RF	Radio Frequency	9
TNO	Netherlands Organisation for Applied Scientific Research	13
EM	Electromagnetic	14
MTI	Moving Target Indicator	15
PPI	Plan Position Indicator	17
ADT	Advanced digital tracker	17
NAIZ	Non Auto-Initiation Zone	19
AGC	Automatic Gain Control	19
M&S	Modeling and Simulation	21

Abbreviation		Page
EW	Electronic Warfare	29
AGL	Above Ground Level	29
EOB	Electronic Order of Battle	48
MSL	Mean-Sea Level	48
TIREM	Terrain Integrated Rough Earth Model	48
IADS	Integrated Air Defense System	52
VTRPE	Variable Terrain Radio Parabolic Equation	53
APM	Advanced Propagation Model	53
SBR	Shooting and Bouncing Ray	54

MODELING AND SIMULATION ARCHITECTURE
FOR STUDYING DOPPLER-BASED RADAR
WITH COMPLEX ENVIRONMENTS

I. Introduction

1.1 Background

The United States Department of Energy set a goal for wind to produce 20% of the US electric generating capacity by 2030 [33]. In 2007, the US cumulative turbine capacity was 16.9 GW, which provided 1% of the total US energy. The US isn't the only country harnessing wind; Germany's cumulative turbine capacity was 22.3 GW. In addition, Denmark has the highest percentage of wind power generation at 20% [36]. The primary method of transforming wind energy into electricity is a wind operated generator, called a wind turbine.

A typical wind turbine is composed of three 40 to 60 m blades connected to a nacelle or gear generation unit which sits on top of an 60 or 100 m tower. Fig. 1.1 shows a picture of a typical wind turbine. The blades rotate from 4 to 15 rpm to produce tip speeds, that is, radial velocities at the tip of the turbine, of over 200 mph. Individual turbines can provide over 1.6 MW of power [21]. Turbines are often arrayed along ridges and plateaus to capitalize on strong winds, a collection of turbines is called a wind farm.

1.2 Problem Statement

One side effect of wind farms is that they can interfere with Air Defense (AD) and Air Traffic Control (ATC) radars because of Doppler effects. The US and UK have each performed several field tests in an effort to characterize the interactions and develop policies for siting wind turbines [25]. As of 2008, the US Department of Defense (DoD) has no formal review process [33], but it does support FAA siting

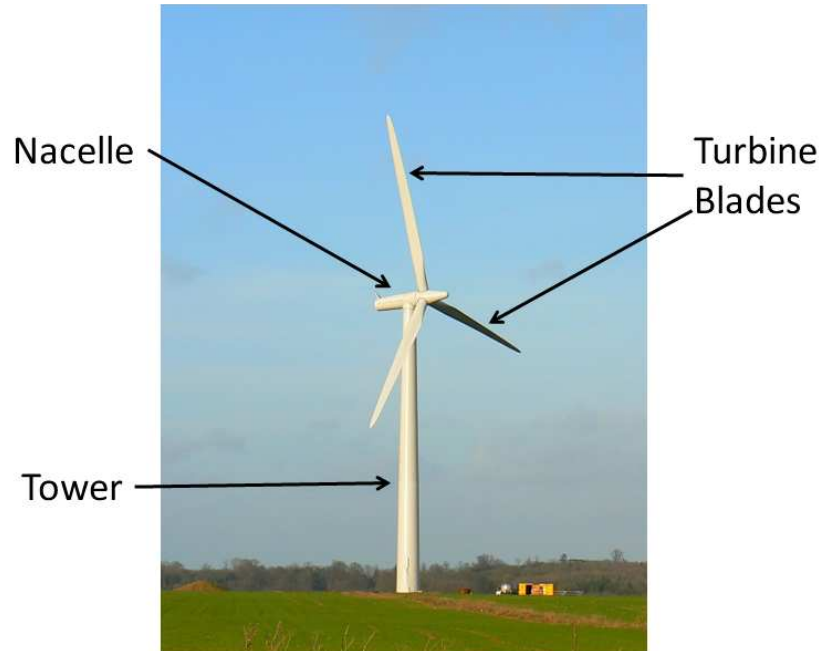


Figure 1.1: The basic components of a wind turbine [23].

studies. One reason for this is a lack of analysis tools for studying wind farm effects on AD and ATC radar performance. A comprehensive tool is needed to analyze the interference effects to aid the U.S. Government in determining optimal locations for new turbine construction.

Interference can be categorized by three effects: false moving targets, degraded target tracking, and missed targets. False moving plots are created by the combination of the turbine's Radar Cross Section (RCS) and the high tip speed from the moving blades. Many radars employ adaptive techniques that change the detection threshold when a large RCS return is present during several scans in an attempt to remove stationary objects. Signals returned from small aircraft are below the new detection threshold, resulting in missed targets. In addition, when a radar is tracking an airplane that flies over or near a wind farm, the radar can select the false plots and lose the track history.

1.3 Proposed Solution

This thesis describes a software architecture including fidelity requirements to model and analyze wind turbine effects on pulse Doppler radar. There are no available programs with sufficient fidelity to evaluate current and future turbine sites. One product of the proposed architecture is the ability to convey the affect of turbines on a combined radar coverage map [11].

1.4 Sponsors

1.4.1 84 RADES. The mission of the 84 Radar Evaluation Squadron (RADES) [3] is “to provide the Warfighter responsive worldwide radar-centric planning, optimization, and constant evaluation to create the most sensitive integrated radar picture.” They are the main DOD organization charged with understanding and evaluating the effects of wind turbines on ATC radars. The proposed modeling and simulation architecture can be used as a baseline to develop software to analyze the effect of wind turbines on a radar. In particular, this effort will determine which components require additional development.

1.4.2 NASIC. The mission of the National Air and Space Intelligence Center (NASIC) [24] is to “produce integrated, predictive air and space intelligence to enable military operations, force modernization and policymaking.” NASIC is interested in modeling advanced sensors and the radar principles involved with wind turbine modeling are very relevant to many sensors studied by NASIC. Hence, recent improvements to a particular modeling and simulation environment, interactive sensor simulator for terrain environments (*INSSITE*), offers a means to study the wind turbine problem.

1.4.3 453rd EWS. The 453rd Electronic Warfare Squadron (EWS) [15] “provides EW-focused Information Operations (IO) analysis, data, flagging, models and simulations to focus combat power, increase survivability and ensure mission success”. One effort of this thesis is to include large objects, like buildings and

wind turbines, within Digital Terrain Elevation Data (DTED). That capability when paired with *Improved Many-On-Many (IMOM)*, a 453rd EWS product, may enhance the accuracy in radar-based wind farm analysis.

II. Literature Review

This chapter will focus on work that others have performed on similar topics, starting with a quick introduction of radar basics. Next is a review of physics effects associated with wind turbines. This is followed by papers that show wind turbines can impact a radar's performance [21]. Finally, the proliferation of large-scale modeling and simulation is discussed.

2.1 Radar Basics

2.1.1 Radar Range Equation. One of the first equations derived in any radar book or paper is the received power,

$$P_r = (P_t G_t) \frac{\sigma}{4\pi R^2} \frac{G_r \lambda^2}{4\pi(4\pi R^2)}, \quad (2.1)$$

where $P_t G_t$ is the transmit power directed towards a target, $\sigma/4\pi R^2$ is the portion of the signal reflected by the target, and $G_r \lambda^2 / (4\pi R)^2$ is the portion of the reflected energy intercepted by the antenna [9] [30]. The $4\pi R^2$ term in the denominators account for spherical radiation. Another important equation is the maximum radar range,

$$R_m^4 = \frac{P_t \tau G^2 \lambda^2 \sigma F^4}{(4\pi)^3 k T_s D_x(n) L}, \quad (2.2)$$

where L is the combined loss factor, F is the pattern propagation factor, and $D_x(n)$ is the detectability factor [9]. The detectability factor is also known as minimum discernible signal [30].

2.1.2 Primary vs Secondary Surveillance Radar. AD and ATC radars typically employ a primary surveillance mode where a RF signal is transmitted into a volume of space and objects in the path reflect the signal. The primary surveillance radar (PSR) processes the returned signals to determine locations. Therefore, PSRs are subject to two-way RF propagation losses, like (2.1).

A secondary surveillance radar (SSR) is a cooperative system with aircraft. ATCs send a coded RF signal and any aircraft equipped with a transponder or beacon sends a coded message back to the SSR. The message from the aircraft contains identification, heading, speed, and elevation information. SSRs are subject to one-way RF propagation losses. SSRs are less susceptible to clutter because of the one-way path loss.

SSRs provide more accurate data than PSRs. However, SSRs use a cooperative system, it is ineffective if an aircraft doesn't have it or isn't using a beacon. For that reason, AD radars depend on PSR to locate any and all targets both friend and foe. Whenever the term radar is used throughout the rest of this document it is referring to PSR.

2.2 *Wind Turbine Physics*

2.2.1 Line of Sight. The first question to ask when determining if a turbine will affect a radar is: Will the turbine be within the radar's line-of-sight (LOS)? LOS can be estimated as

$$D = 1.41[\sqrt{h_t(ft)} + \sqrt{h_r(ft)}] \text{ miles}, \quad (2.3)$$

where, h_t is the height of the turbine, and h_r is the height of the radar above mean sea level [21]. The equation assumes a 4/3 earth radius to account for beam diffraction [21]. The result is a minimum separation distance required to ensure the turbine won't interact with the radar.

However, (2.3) doesn't account for terrain masking or shadowing. If there is a tall object or terrain between the radar and the turbine, the LOS distance may be shorter [14] [21]. Figure 2.1 illustrates how diffraction increases the radar coverage beyond the visible region. Some models, such as *IMOM*, account for terrain masking and beam diffraction around terrain to provide range detection diagrams [13].

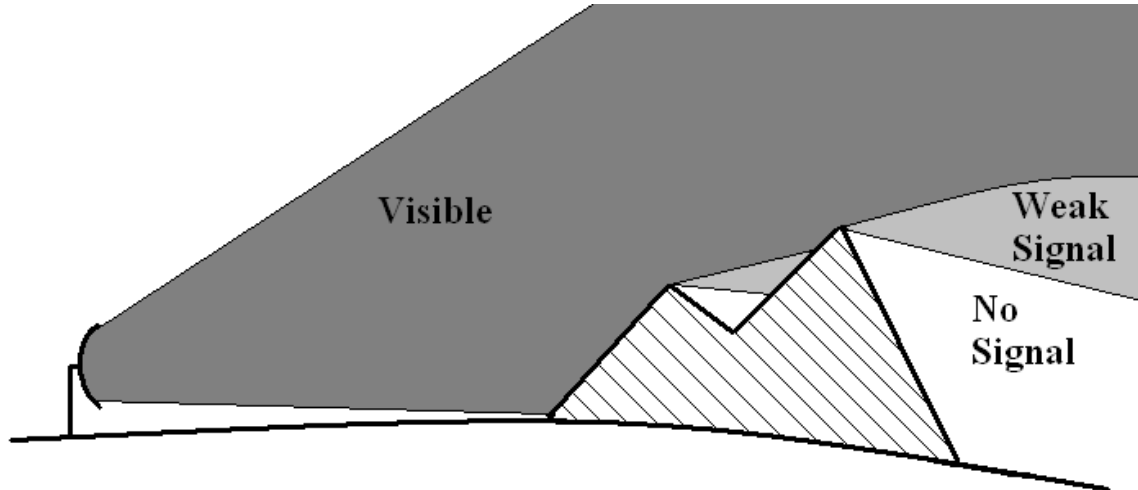


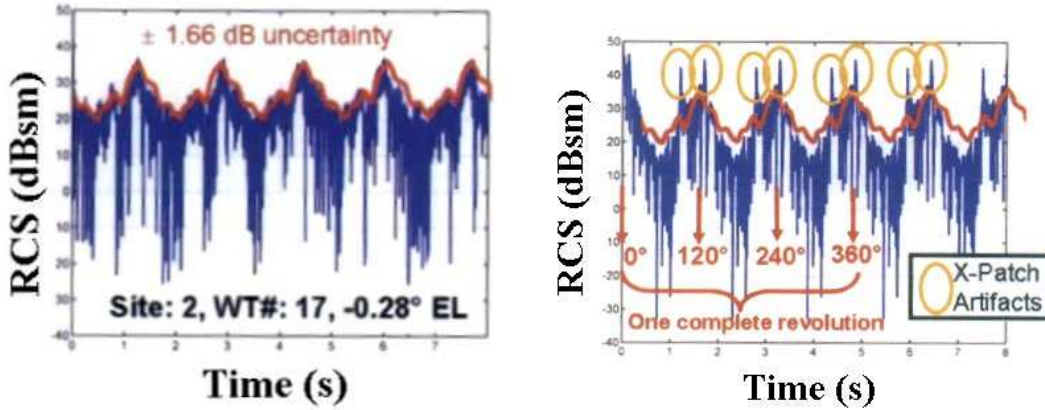
Figure 2.1: Depiction of diffraction from terrain. The regions in light grey are partially visible because of diffraction.

2.2.2 Radar Cross-Section. The σ term in (2.1) is the RCS of a target. RCS is a measure of an object’s scattering magnitude [20]. A common misconception is that RCS is constant for an object, when it actually depends on many factors, including object orientation and radar wavelength.

Numerous books, like Knott [20], are dedicated to explaining methods for computing RCS values. Methods range from coarse and quick which provide simple values to detailed and time intense, like *X-Patch*. The quick methods rely on multiple assumptions to calculate values. Decreasing the number of assumptions and increasing the density of the observation grid will increase the accuracy, complexity, and time of the calculations. Accuracy and timing requirements will determine what methods can be used to model turbine RCS.

Wind turbines are very large electrically, meaning they are on the order of several hundred wavelengths tall [19]. The following is an example of pre-processed RCS approximation method that could be leveraged to reduce evaluation time of a wind farm.

The RCS of a turbine, using a computational electromagnetic (CEM) program like *X-Patch* with a fine computational mesh at X-Band, can take over a decade for a



(a) The measured RCS of the GE windmill (170 deg yaw, 0 deg elevation, 1.5 GHz, 12.7 rpm, VV polarization) [19].
 (b) The predicted RCS of the GE windmill (170 deg yaw, 0 deg elevation, 1.5 GHz, 12.7 rpm, VV polarization) [19].

Figure 2.2: Measured vs *X-Patch* RCS [19]. The diagram in 2(a) shows the measured RCS of a wind turbine ranges from 40 dBsm to 20 dBsm. On average, 2(b) shows the predicted RCS matches actual measurements. However, the spikes, in 2(b) are artifacts of the simulation.

64-node supercomputer to process [19]. That calculation accounted for 120° of blade rotation. For lower frequencies, such as L- or S-Band, a coarse mesh is used to reduce computation time without sacrificing accuracy. The density and size of the mesh directly influences the processing time. Another drawback is these calculations would need to be performed and stored for every wind turbine model used in the US, or a reasonable subset. But once a model has been evaluated, the data can be accessed via look-up tables.

The Air Force Research Laboratory (AFRL) performed field tests with 10 turbines in Fenner, NY. The turbines were evaluated at L-, S-, C-, and X-bands with a variety of wind conditions to characterize RCS and Doppler characteristics [25]. The goal was to create a data set to verify RCS simulations of turbine models. Figure 2(a) shows the actual measured data and Figure 2(b) shows the simulated *X-Patch* results [19]. The simulation data closely matches measured data except for the artifacts.

2.2.3 Doppler Effect. The Doppler effect is the compression or expansion of radio frequency (RF) signals by a moving object. Pulse Doppler radars can measure the frequency change or Doppler shift of the transmitted signal. These radars use the Doppler shift to calculate how fast an object was moving. This relationship is described by

$$f_d = 2\frac{v_r}{\lambda}, \quad (2.4)$$

where f_d is the Doppler shift, v_r is the radial velocity, λ is the wavelength of the transmitted signal [30].

The wind drives the turbine blades, which are connected to a generator by a shaft, to rotate and generate electricity. Figure 2.3 depicts a power curve for a turbine [8]. As the wind speed increases, the turbines rotate faster producing more power and a larger Doppler shift. Figure 2.4 shows tip speed relative to wind speed for several common wind turbine models [8]. At maximum rotation speeds, the turbine is comparable to a slow flying aircraft.

The Doppler returns from a turbine are well documented by QinetiQ [26] and AFRL [4]. Figure 2.5 is an example of the Doppler returns created by a wind turbine [26]. The wind is blowing perpendicular to the radar boresight creating maximum Doppler shifts. The cyclical spikes in Doppler correspond to times when the turbine blade is passing either straight up or straight down. A smaller spike forms just before or just after a turbine blade passes vertically downward. The smaller spike is caused by the combined blade and tower phase center moving rapidly away from the radar [26].

Another factor that determines the Doppler shift the radar perceives is the angle between the turbine blades and radar boresight. The equation for calculating the maximum Doppler shift caused by turbine blades is

$$f_d = 2\frac{wr}{\lambda}|\cos(90^\circ + \phi_{radar} - \phi_{wind})|, \quad (2.5)$$

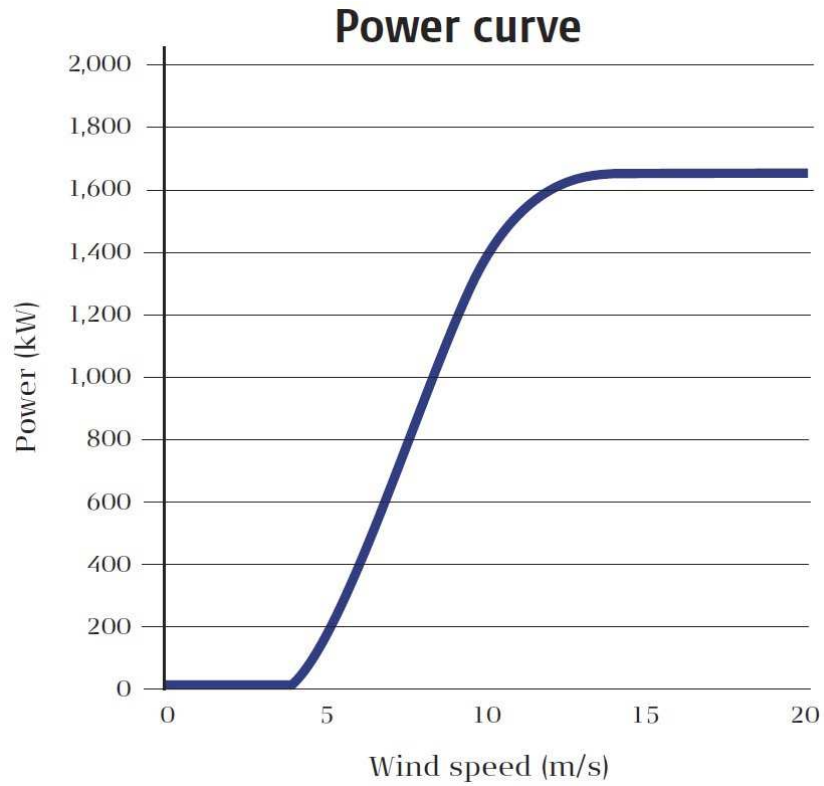


Figure 2.3: The graph depicts typical power curves for wind turbines vs wind speed [34]. Turbines usually produce little to no power for low wind speeds then increase linearly for normal operating ranges before reaching a max power plateau.

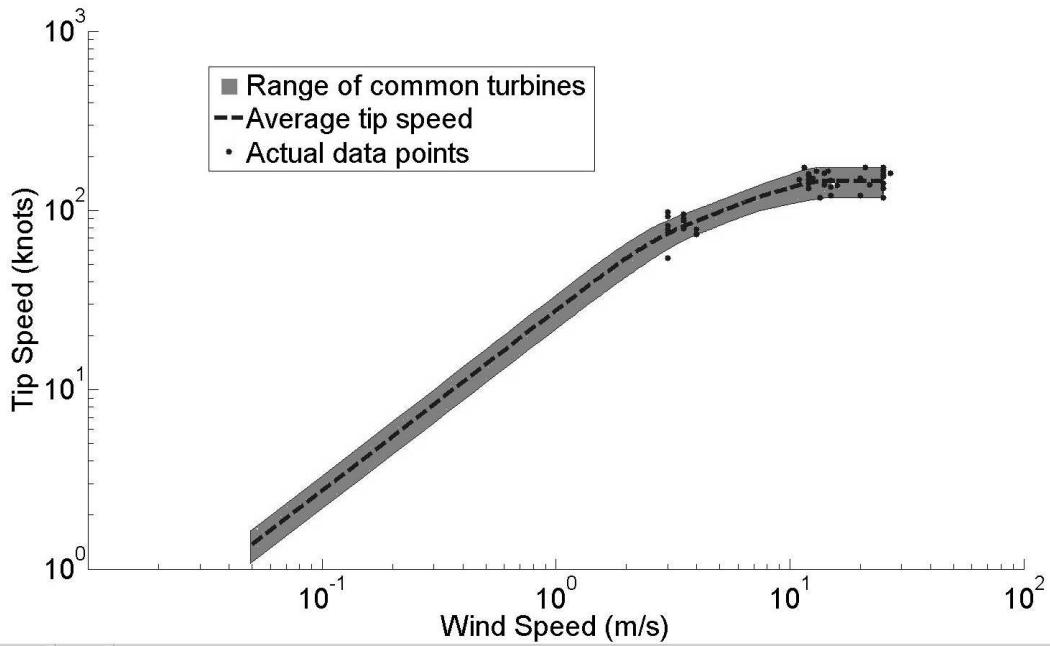


Figure 2.4: The graph shows estimated tip speed vs wind speed for common wind turbines [8].

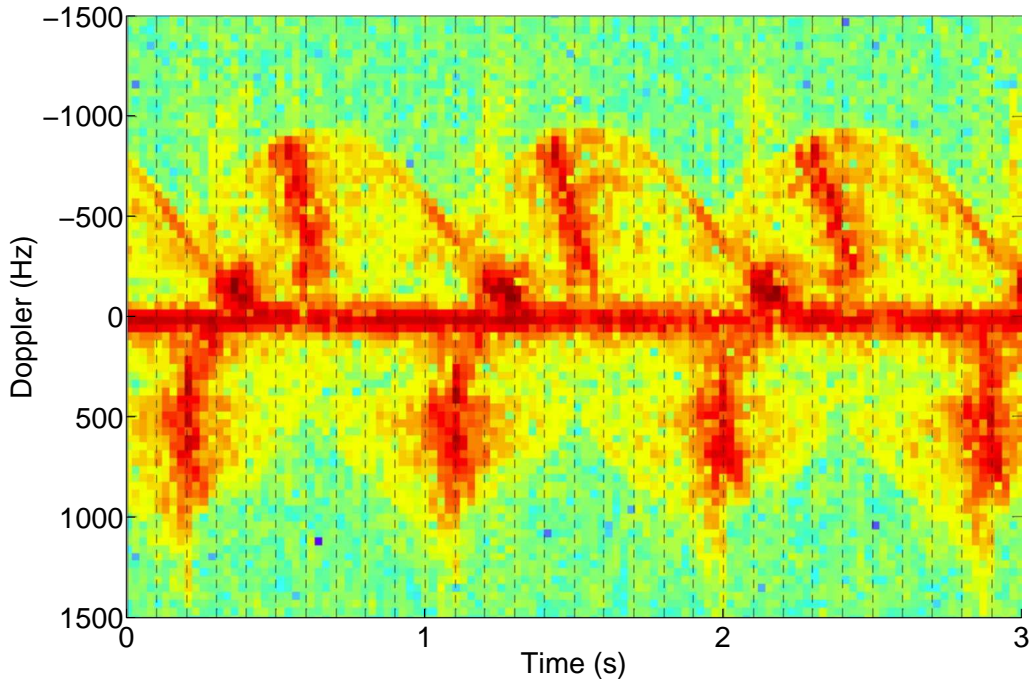


Figure 2.5: The graph illustrates the cyclical Doppler returns from a wind turbine [26].

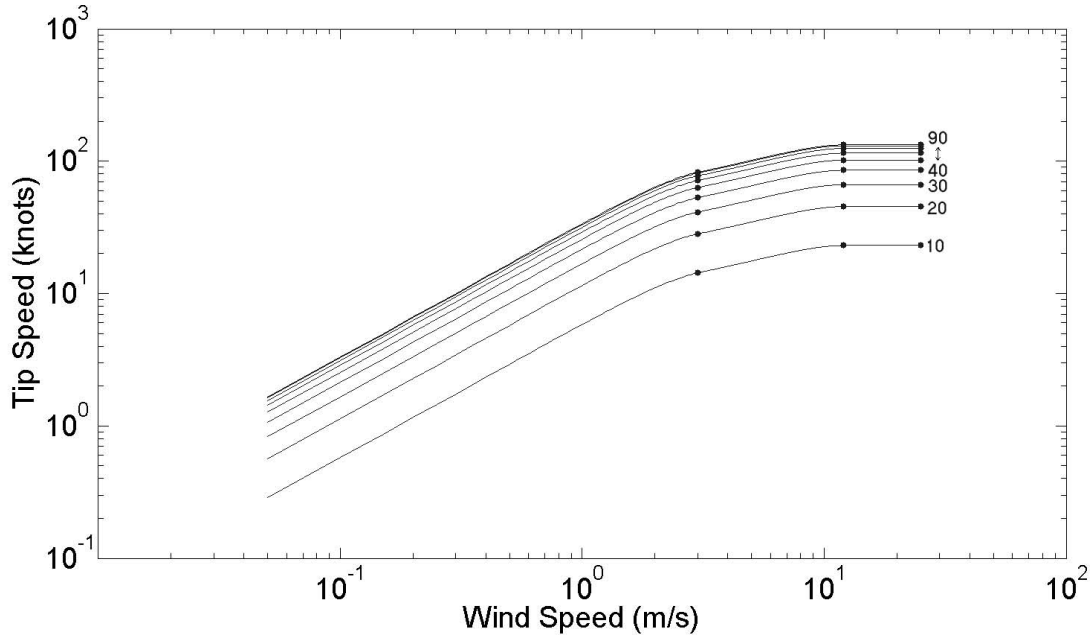


Figure 2.6: Family of curves showing apparent tip speed as wind changes direction by 10 deg increments [8]. The apparent tip speed decreases as the angle approaches 0, when the blades are facing the radar.

where r is the length of the blades in meters, w is the rotation rate of the blades in RPM, λ is the operating frequency of the radar, ϕ_{radar} is the radar azimuth (measured from North), ϕ_{wind} is the wind direction, and the 90 deg factor accounts for turbine blades spin perpendicular to wind direction [8]. The equation reaches the maximum value when $\phi_{radar} - \phi_{wind}$ is an odd multiple of 90 deg. Figure 2.6 shows a family of curves for apparent tip speed versus wind speed for a single wind turbine based on the angle between radar boresight and wind direction [8]. That means false targets that move tangent to the boresight of the PSR will appear much slower than inbound or outbound false targets which may have implications for tracking algorithms.

2.3 Wind Turbine Effects on Radar

Shadowing is the largest concern for AD radars [13]. Table 2.1 shows the significance of each impact depends on the radars use [13]. The terms “Raised Threshold” and “Clutter” are related because a radars’ detection threshold is raised to reduce clutter [13].

Table 2.1: Order of significance for PSR impacts, 1 is highest [13]

Impact	Type of Airspace/Use of PSR			
	Airport/Approach	TMA/High Density En-Route	Low Density En-Route	Air Defence
Shadowing	3	3	2	1
Clutter	1	1	1	3
Raised Threshold	2	2	3	2
Receiver Saturation	4	4	4	4

2.3.1 Shadow Zone. In the same manner that terrain can mask wind turbines, turbines can also mask targets. The region behind a turbine, from a radar’s perspective, that is either completely or partially occluded is called a shadow zone. The UK flight test determined that the shadow zone would affect a PSR’s ability to detect targets within 5 km behind a wind farm [5].

A shadow zone usually forms a 4 deg or smaller wedge behind large obstructions like turbines [14]. The two-way reduction in power [21] caused by shadowing is

$$L_{sz}(dB) = 40 \log \left(1 - \sqrt{\frac{D_{rt}S^2}{D_{rw}D_{wt}\lambda}} \right), \quad (2.6)$$

where D_{rt} is the distance between radar and target, D_{rw} is the distance between radar and wind turbine, D_{wt} is the distance between wind turbine and target, and S is the width of the wind turbine. The greatest reduction in power happens when the target is directly behind and in line with the wind turbine. The farther apart the target and the wind turbine are, the smaller the shadow zone affect on probability of detection. Diffraction is the primary reason that the partial shadowing has less effect on radars at longer separations. Table 2.2 provides rule-of-thumb values for shadow length, based on acceptable power loss [14].

The Netherlands Organisation for Applied Scientific Research (TNO) also investigated radar shadowing [31]. TNO focused on reducing maximum detection range and probability of detection. They determined that placing a turbine 4 km to 8 km

Table 2.2: L-Band (1 GHz) rule-of-thumb shadow length values. The values are the distance (km) the shadow extends behind the turbine. [14]

Tolerable power loss PL (dB)	Distance from radar to turbine (km)					
	0.5	1	2	5	10	20
0	∞	∞	∞	∞	∞	∞
-1	∞	∞	∞	46.0	8.2	5.8
-2	∞	∞	3.4	1.7	1.4	1.3
-3	∞	1.7	0.9	0.7	0.7	0.6
-5	0.6	0.4	0.3	0.3	0.3	0.3
-10	0.1	0.1	0.1	0.1	0.1	0.1

away from the radar reduces the maximum detection range [31]. In addition, they showed that for a 1 m² target, the detection probability from a single dwell is reduced by as much as 40% when a turbine is placed 4 km from the radar, which is quite significant. TNO didn't supply results for cases where turbines were 30 km or more away from the radar, which is more common in the US.

Shadow zones are predictable which leads to a simple mitigation technique. The technique is to site turbines at the base of plateaus or on hillsides, ensuring a portion of the shadow zone is masked by terrain [14]. Figure 2.7 is a hypothetical scenario that applies this method. The dashed area is the profile of the shadow zone. In effect, this approach overlaps areas the radar can't view.

2.3.2 Clutter. Clutter is unwanted scattered signals from trees, birds, rain, sea, ground, buildings, and other large structures [9]. Wind turbines are large metallic structures that fall under the category of clutter, the combination of size and electromagnetic (EM) properties result in strong radar returns. To put the size in perspective, the RCS of a 1.6 MW wind turbine can average between 20 and 40 dBsm which is comparable to a passenger jet aircraft [25]. The rated power output of a turbine increases directly with blade length and generator efficiency, but the turbine's RCS scales with the size of the tower and blades.

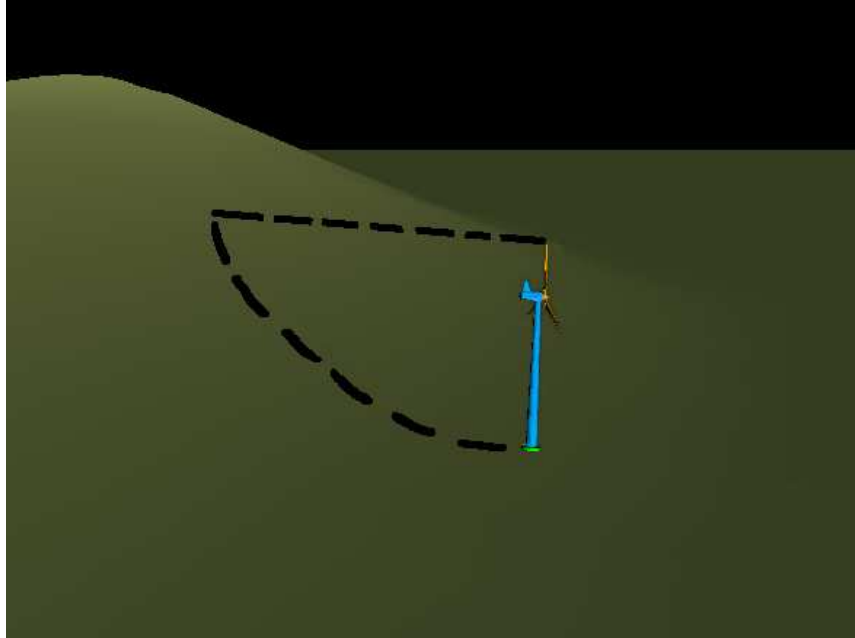


Figure 2.7: The dashed line represents a shadow zone being clipped by terrain.

2.3.3 Raised Threshold. Modern radars use clutter maps to isolate and remove stationary clutter. Clutter maps are divided into clutter cells which can be further divided into range resolution cells. Figure 2.8 compares 9 range resolution cells that cover 3 km in range and 3 deg in azimuth with a clutter cell that is 3 km in range and 3 deg in azimuth [25]. The radar keeps a history of the signal strength for several scans and adjusts the detection threshold of each clutter cell. A large scatterer in one range cell will cause the detection threshold of neighboring range cells, within the clutter cell, to also increase [7]. A turbine in cell A can mask a target in cell B.

Figure 2.9 shows the affect of turbine farms on AD radar clutter maps [7]. The thick lines are the clutter cell; cells A10, B10, and B11 contain turbines. In those cells, the PSR returns from the aircraft are below the detection threshold and only SSR returns were received.

2.3.4 False Moving Targets. Moving target indicator (MTI) circuits remove stationary clutter. If a target is stationary, the successive pulses are nearly identical

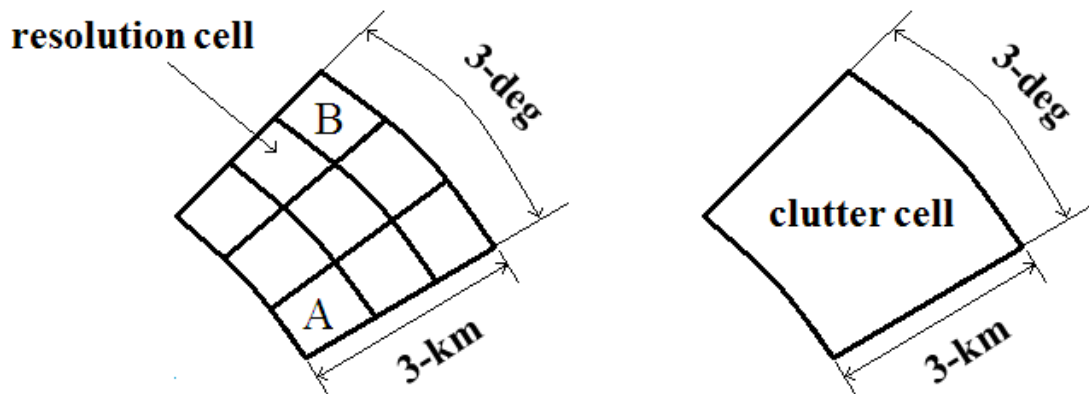


Figure 2.8: Clutter cells are generally the size of multiple range resolution cells.

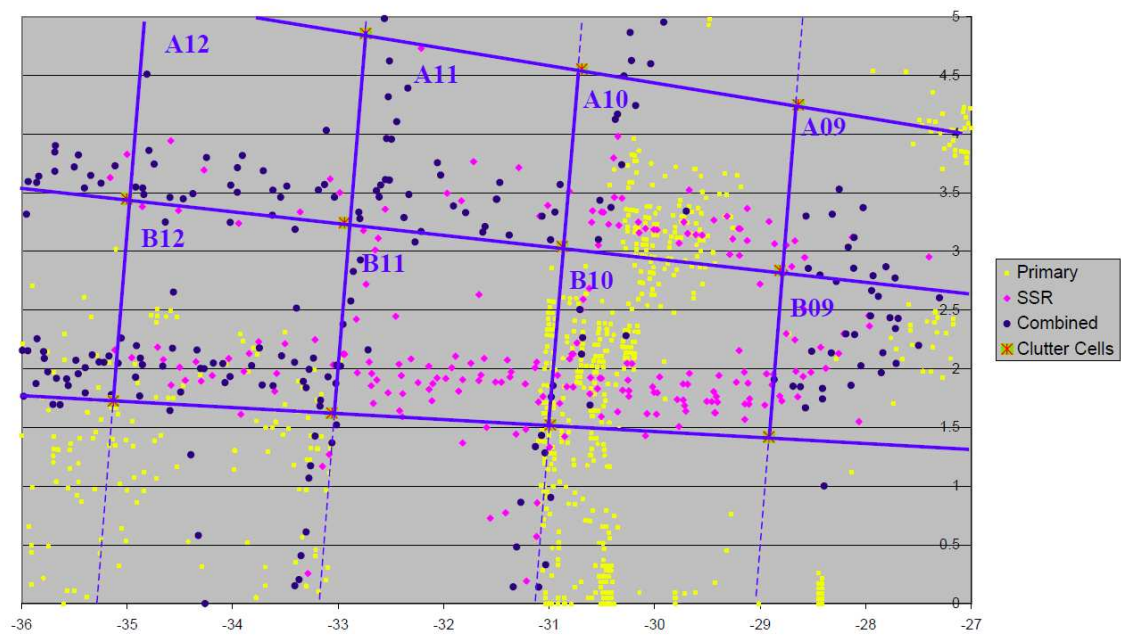


Figure 2.9: Data from a flight test showing clutter cells that contain wind turbines (A10, B10, and B11) have a reduced probability of detection [7].

Table 2.3: L-Band (1 GHz) rule-of-thumb RCS values [14]

Blade length (m)	Typical maximum pre-MTI RCS (dBsm)	Typical average pre-MTI RCS (dBsm)	Typical maximum post-MTI RCS (dBsm)	Typical average post-MTI RCS (dBsm)
60	54	44	53	9
55	53	43	52	8
50	51	42	51	7
45	50	41	50	6
40	49	40	48	5
35	47	39	46	4
30	45	38	44	3
25	43	36	42	1
20	40	35	39	0
15	37	33	35	-2
10	33	31	29	-4
5	29	29	18	-6

and will cancel out when subtracted. However, moving objects cause pulse-to-pulse phase changes that are not canceled by MTI circuits. Subsequent Doppler filters are needed to estimate the target's velocity [25].

MTI filters can remove part of the turbines radar return, e.g. from the stationary tower, and thereby reducing the average return energy, as shown in Table 2.3. There are additional rule-of-thumb tables for S- and X-Band in [14]. The combination of long turbine blades and high rotation rates results in tip speeds that are comparable to slow flying aircraft (180 mph) [25]. The correlation of a large radar return and Doppler shift from the turbine blades will insure radar returns pass through MTI filters as valid targets for display on a plan position indicator (PPI). Figure 2.10 shows a PPI display where wind farm clutter is indistinguishable from a moving aircraft [6].

There are no current techniques that can filter the returns from a moving turbine without adversely affecting desired aircraft returns, but one is being developed by BAE [14]. Advanced digital tracker (ADT) reduced adverse impacts caused by wind turbines on radar [12]. However, some tracks were dropped and other tracks were

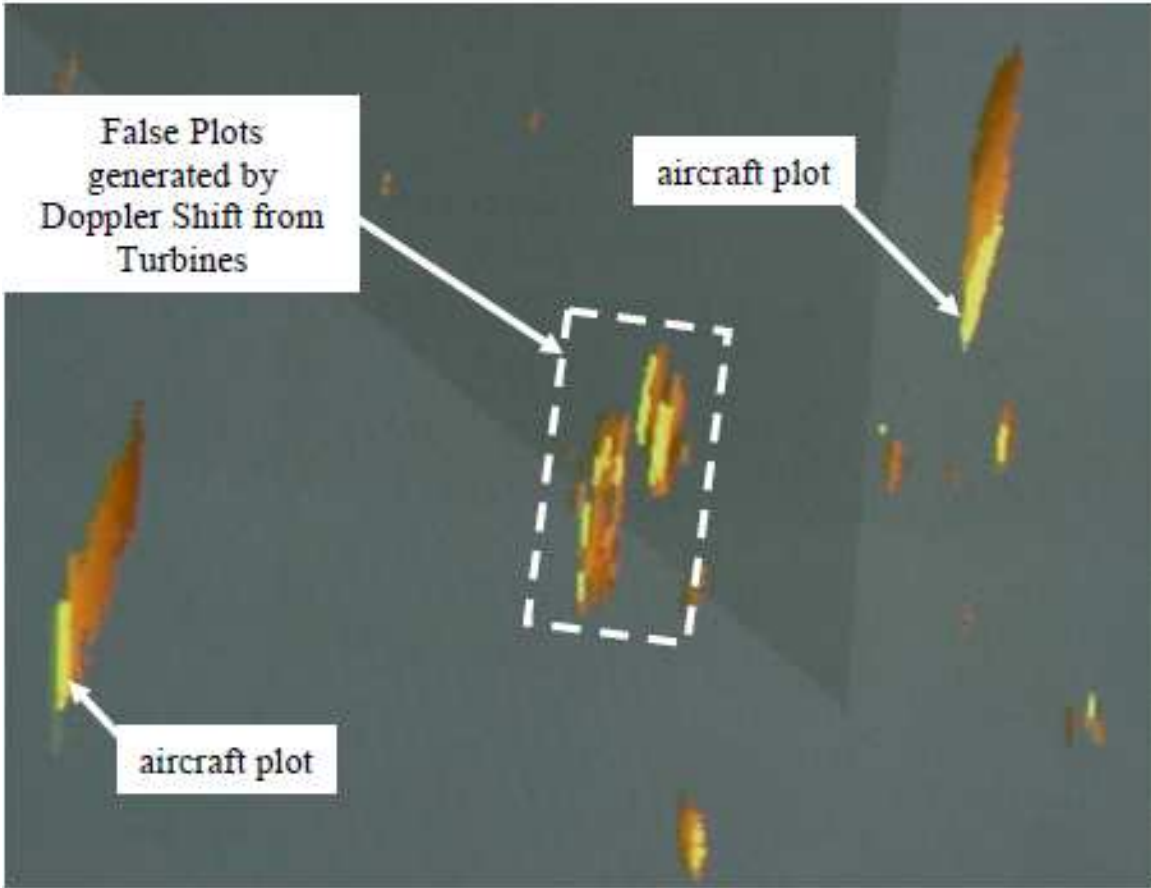


Figure 2.10: Plan position indicator (PPI) [6] showing how difficult it is to distinguish a turbine from an aircraft.

seduced [12]. In 2006, the UK Ministry of Defence determined the product didn't completely mitigate safety concerns [12].

2.3.5 Tracking. Radar target tracking is accomplished by first estimating a target's current range and velocity and then estimating where the target will be at the next scan and selecting a correlation gate to pick up the next return. If there are multiple moving targets within a correlation gate, the tracker has to decide which return belongs to which track. When a situation like that occurs, the tracker can either select the right target/track pairing, switch the tracks, or drop the tracks altogether and start new tracks. Tracking radars usually have a "limited" number (several hundred to several thousand) of targets they can simultaneously track. The hardware processing power limits the number of target tracks available.

Wind farms can severely degrade a tracking radar's performance, based on turbine layout and spacing [14]. The false moving targets can lure the tracker away from the real target, and the raised detection threshold can mask returns causing a track to drop. In addition, wind farms may be capable of producing enough false plots to overwhelm the tracking processor, causing the radar to drop tracks or stop initiating new ones.

One mitigation technique for trackers, called non auto-initiation zone (NAIZ), allows operators to establish zones where no new tracks will be created [14]. Tracking radars that use NAIZ will assume aircraft fly straight over a wind farm. Because of that, the tracker will coast the track and attempt to reacquire the aircraft once it clears a farm, thereby preserving track history. However, trackers that use NAIZ still can't reliably track an aircraft over a wind farm.

2.3.6 Receiver Saturation. Saturation occurs when large objects are near the radar, resulting in large amplitude returns which saturate the receiver [13]. Receiver saturation is one effect that is often neglected in modeling and simulation, because many radars employ automatic gain control (AGC) to prevent saturation. When a

Table 2.4: Proposed Wind States [8].

Tip Speed (kts)	Wind State	Approximate Wind Speed (m/s)
$0 < v_r \leq 20$	0	1
$20 < v_r \leq 40$	1	2
$40 < v_r \leq 60$	2	3
$60 < v_r \leq 80$	3	5
$80 < v_r \leq 100$	4	7.5
$100 < v_r \leq 120$	5	10
$120 < v_r \leq 140$	6	13
$140 < v_r \leq 160$	7	17
$160 < v_r \leq 180$	8	22
$180 < v_r$	9	25+

receiver is saturated, the sensitivity and dynamic range are reduced, which reduces the radar’s maximum detection range.

2.4 Modeling Wind Turbine RCS

As shown previously, performing CEM on wind turbines is expensive in both time and resources. When you combine the fact that there are a vast amount of turbine manufacturers and many have multiple models that would need to be computed, a method using look-up tables seems unlikely in the near term.

Another method for modeling wind turbines is a concept called wind states [8] which uses stochastic amplitude and phase data to describe wind turbine clutter. A similar concept, the notion of sea states effecting sea clutter, is widely used in radar receivers [8]. Table 2.4 associates wind states with ranges of tip speeds [8].

The proposed signal model

$$s(t) \propto \langle \sigma_\theta \rangle e^{j\langle \phi_\theta \rangle} s_0(t), \tag{2.7}$$

where $s_0(t)$ is the signal when modeled with the radar range equation, $\langle \sigma \rangle$ and $\langle \phi \rangle$ are the magnitude and phase of turbine clutter [8]. Aircraft returns and ground clutter

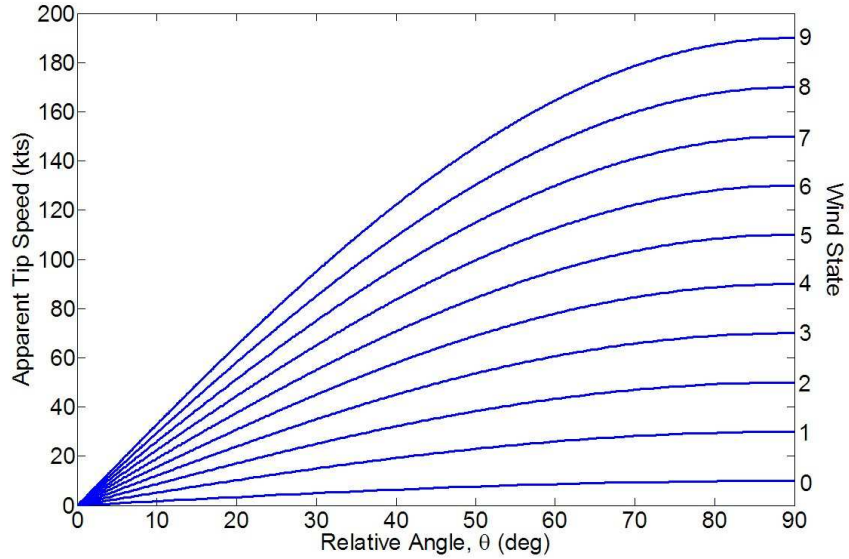


Figure 2.11: Maximum Doppler versus angle between radar boresight and wind direction based on (2.5). The graph accounts for varying wind states.

are accounted for in $s_0(t)$. Stochastic methods produce accurate data quickly without requiring the use of supercomputers.

The goal of wind state modeling [8] is to create a family of curves similar to probability of false alarm graphs for receivers [30]. Figure 2.11 displays a hypothetical graph of maximum Doppler versus angle for various wind states. Figure 2.12 shows how $\langle \sigma_\theta \rangle$ might be calculated from a collection of turbine measurements.

2.5 Large Scale Modeling and Simulation

2.5.1 How Large is Large? The definition of large-scale modeling and simulation (M&S) varies from one source to another. One of the generic definitions is, any system that can be separated into a number of interconnected subsystems for either computational or practical reasons [18]. Another definition is, the dimensions of the system are so large that conventional techniques of modeling, analysis, control design, and optimization fail to give reasonable computational efforts [18]. That can be simplified to “a system is large when it requires more than one controller” [22].

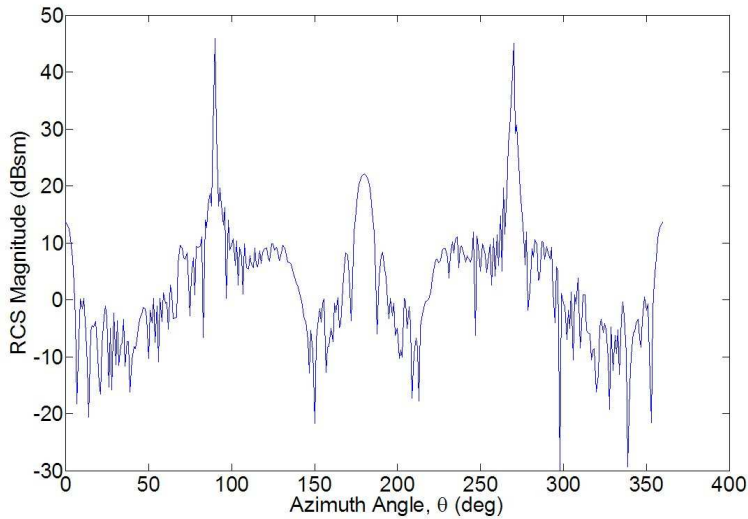


Figure 2.12: Example using a collection of turbine measurements with multiple blade positions to generate $\langle \sigma_\theta \rangle$.

2.5.2 Who Uses Large-Scale M&S? In short, almost everyone. Large-scale models and simulations are hierarchical, decentralized information structures that approximate systems dealing with society, business and management organizations, the economy, the environment, communication, electrical power, logistics, military command and control, information systems, aerospace, water resources, and energy [18]. Therefore, modeling the effects of turbines on a radar, in detail, would qualify as a large-scale model.

Both the government and contractors have developed many large-scale M&S applications to simulate radar-aircraft-clutter interactions. This report will focus on two applications, SAIC's *INSSITE* and the 453rd's *IMOM*. In addition, these applications will be evaluated for their potential to model radar-turbine-aircraft interactions in the following chapters.

2.5.3 M&S Hierarchy. One method for defining the layers of a model or simulation is shown in Fig. 2.13 [28]. The bottom layer is physics, which controls physical interactions and phenomena, like EM radiation and aircraft kinematics. The physics-layer is not computationally expensive for a small scenario, and there is almost

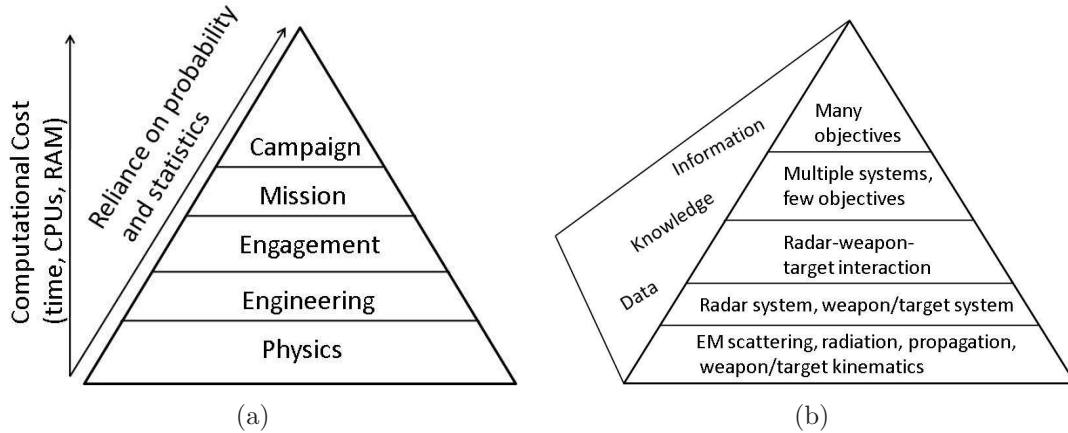


Figure 2.13: Modeling and simulation pyramid. (a) Cost versus level of representation. Physics models have the highest-level and most accurate representation. Campaign models have the most reduced form and often depend on significant statistical analysis. (b) Data, information, knowledge versus pyramid level. Knowledge requires the greatest amount of processed information, which means higher costs [28].

no dependence on probability or statistics. The top layer is campaigns, which are vast scenarios encompassing many objectives or missions. An example is evaluating the effect of turbines on the US combined radar coverage map. Campaign models are supported by running well-over a thousand iterations of a simulation to develop the probability and statistics information. Therefore, vast resources are needed to generate results at the campaign level.

On the side of Fig. 2.13(b) there are three words: data, information, and knowledge. Data is often viewed as the “lowest level of abstraction from which information and knowledge are derived” [35]. Information is “giving form or shape to the mind, as in education, instruction, or training” [29]. Information can also be thought of as refined data, but information is not always accurate [35]. Knowledge is “what is known in a particular field or in total; facts and information” [29]. Every layer of the pyramid can contain data, information, and knowledge [28].

Figure 2.14 shows military planning is very similar to the M&S pyramid [32]. Along the bottom is complexity which is synonymous with computational cost. In addition, the focus of effort scale ranges from designing (art) which seeks a systemic

III. Methodology

This chapter covers the method used to develop the modeling and simulation framework for analyzing the effect of complex clutter on a pulse-Doppler radar. Two programs will be run through several set scenarios to create baseline capabilities for future simulation software.

3.1 Overview

Figure 3.1 depicts the method that was followed to generate a M&S architecture. The first step, understand the problem, was detailed in Chapters I and II. For the second step, determine the components, the high-level systems were obvious: radar, aircraft, turbines, terrain, and EM phenomenon. Some of the systems can be separated into logical subcomponents. Calculating the complexity means evaluating the computational cost of systems at several M&S levels. The evaluation includes computing time and accuracy for every level. At this point a reasonable architecture can be developed. The framework is presented in Chapter IV. Next, two different programs, *INSSITE* and *IMOM*, will be examined in the context of the M&S framework to determine which components are currently developed. The results of the evaluation are detailed in Chapter V. Finally, develop requirements will highlight components that aren't at the appropriate M&S level. The requirements will demand additional data for the development of statistical models.

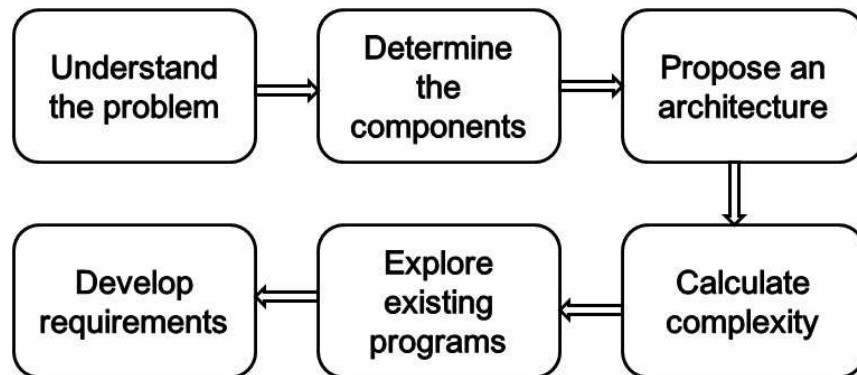


Figure 3.1: Represents the method used to address the problem.

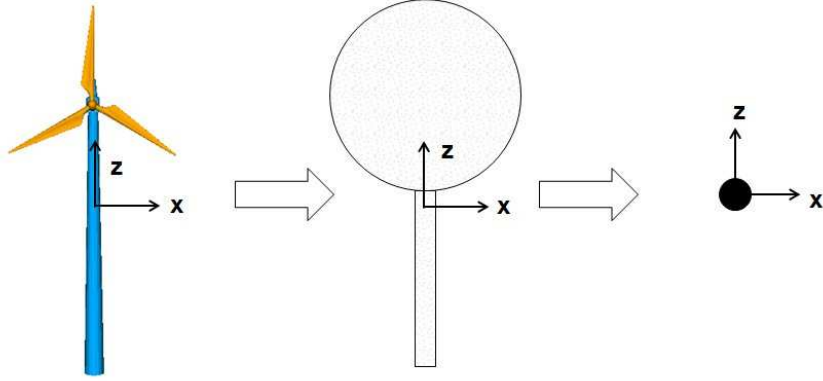


Figure 3.2: The left model can contain 400k or more facets and require more than a year to produce the best representation of one turbine’s RCS. The middle model is a reduction of the left model, it can contain 330k scatterers but only require hours to process a single set. The right model is as simple as possible. It is accurate for a very limited scenario but it’s easy to process.

3.2 Evaluating Complexity

The turbine RCS was evaluated at the physics, engineering, and engagement levels. The evaluation included a physical representation, a method, and a sample model for acquiring RCS. Figure 3.2 illustrates the complexity of three methods used for evaluating turbine RCS. A similar breakdown can be performed for phase data.

3.2.1 Physics-Level. Each individual turbine is represented in extreme detail, thousandths of a degree blade rotations. Several methods: method-of-moments (MoM), scattering centers, and ray tracing, are used to generate RCS values at thousands of look angles. They solve very large systems of equations using matrix inversion which has a complexity on the order of N^3 . The method used to calculate the scattered electric field is

$$\bar{E}^s(t, \bar{r}) = \int_v G(\bar{r}, \bar{r}') \bar{J}(t, \bar{r}) d\bar{r}', \quad (3.1)$$

where \bar{r} is the vector from the origin to the observation point, \bar{r}' is the vector from the origin to the source, t is time, G is the Green’s function, \bar{J} is the current density, and \bar{E}^s is the scattered field which can be converted to RCS.

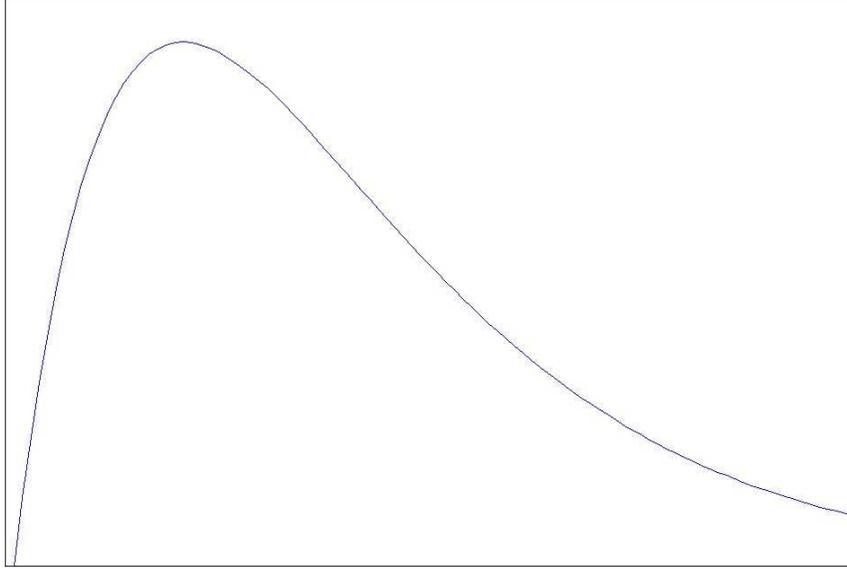


Figure 3.3: Chi-squared function which may simulate the RCS of a turbine. The actual model will need to be derived from physics or engineering-level data.

3.2.2 Engineering-Level. Individual turbines are represented by a set of fixed of blade positions, on the order of degrees. Instead of performing a full physics estimation, look-up tables or a reduced number scattering center models are used. These methods are advantageous because their complexity is on the order of N compared with N^3 for physics methods. When evaluating scattering centers, the total RCS

$$\sigma = \left| \sum_i^N \sigma_i e^{-j\bar{k} \cdot \bar{r}_i} \right|, \quad (3.2)$$

where \bar{k} is the angular wavenumber and σ_i is the RCS from the i^{th} range cell.

3.2.3 Engagement-Level. Whole wind farms are evaluated at this level and blade position is account for statistically. The RCS is generated from a probability density function. A hypothesis test is performed to determine if the radar returns from wind farms are above detection thresholds. This method involves solving one equation which makes the complexity on the order of 1. The model is a graph, similar to chi-squared function shown in Figure 3.3

3.3 Architecture Development

The first step to developing a hybrid large-scale M&S framework is to determine the simulation scope. The scope can be expressed in terms of the M&S pyramid based on the number and scale of the objectives and products. The top-level objective is to simulate the effects of turbine and clutter interference on a radar's ability to detect an aircraft. The next step is to recursively divide the model into logical components or subsystems. Then, define the products and outputs for each component. In addition, the subsystems should be separated based on the fidelity requirements. The final step is to associate the subsystems with particular M&S levels based on its objectives, products, and fidelity. The key to a hybrid model is the ability to access low-level, physics-level, data when required while still being able to use higher-level, engineering or engagement-level, information or knowledge when appropriate.

3.4 Existing Programs

This is not the first modeling architecture ever developed for radar applications. Most radar models use either detailed RCS measurements, like CEM techniques, or a constant amplitude for RCS, ignoring Doppler. CEM and scattering center techniques are prohibitive because of the sheer size of the scenario. A single turbine is electrically very large at typical radar wavelengths. Whereas using a constant amplitude for RCS overly simplifies EM phenomenon and results in important information being lost.

There are a large variety of government and contractor radar models, each tailored for specific purposes. This effort is based on two such programs, SAIC's *INSSITE* and the 453rd EWS's *IMOM*. *INSSITE* operates as an engagement-level simulation with components at the engineering and physics-levels. *IMOM* operates as a campaign or mission-level simulation with subsystems at the engineering and physics-levels.

The programs will be evaluated by reviewing program documentation, creating experimental simulations, and corresponding with program experts. Since *INSSITE*

is an in-house design tool there is little documentation. That means discussions with the program developers will provide a bulk of the understanding of capabilities and limitations. *IMOM* is a prolific program in the electronic warfare (EW) community and is distributed with detailed documentation.

The programs are expected to provide partial solutions for analyzing radar-aircraft-turbines-clutter interactions. As such, the programs might verify some subsections of the proposed framework. However, neither program is likely to provide a complete solution, which led to the design of a hybrid large-scale M&S framework.

3.5 Experimental Simulations

The programs will run through a series of iterative simulation scenarios to determine their strengths and weaknesses for modeling this problem. The experiments will be slightly different for each program due to software limitations.

3.5.1 IMOM Experiments. The main limitation of *IMOM* is that it doesn't calculate phase data. However, it is very effective at calculating the magnitude of returns from targets while also accounting for LOS.

The first experiment is to verify that LOS is taken into account. A radar, with parameters similar to an ARSR-4, will be placed on a plateau and attempt to detect a 1 m² calibration target 200 ft above ground level (AGL). The resulting analysis should show which areas were masked by terrain and which areas were visible.

The second experiment is to test the radar's ability to detect an aircraft while accounting for terrain clutter. The setup is similar to the first experiment except a larger, possibly a 3D, RCS is used and the aircraft is at a higher altitude: 1500 ft AGL. The clutter is incorporated with the various detection methods.

The third experiment is to determine if the radar can detect wind turbines with ground clutter. Again, this is a similar analysis to the first experiment except using

a much larger 10,000 m² RCS. It is anticipated that the radar will detect the turbine at an extended range compared to the calibration target.

The fourth experiment is to combine the second and third test to determine if the radar can detect an aircraft in the same resolution cell as a turbine. However, *IMOM* evaluates each target individually, requiring other techniques to account for the effect of wind turbine clutter on a radar. One possible method involves modifying DTED at the turbine location to increase the terrain clutter. Another method might be to model the turbine as a radar jammer which would raise the radar's detection threshold in a similar manner.

3.5.2 INSSITE Experiments. *INSSITE* is a SAIC in-house development tool that provides some unique features, like the ability to simulate the movement of objects prior to performing detailed analysis. But, the tool is not ready for main-stream use due to some key limitations, like scenario size and sluggish response to user manipulation.

The first experiment is to setup a radar to collect ground clutter. This task will include creating a stationary radar with a rotating beam and incorporating DTED into *INSSITE*.

The second experiment is to place a stationary turbine in freespace, then run analysis with varying observation densities, from 1 λ up to 5 λ , to determine convergence. The objective is to find the largest grid spacing that still produces an accurate RCS magnitude for the turbine. With larger grid spacing, fewer rays are traced, and the processing time is shorter.

The third experiment is to evaluate the RCS of a turbine when combined with terrain. Using a higher multi-bounce setting will provide more accurate data at the expense of simulation time.

The fourth experiment is to calculate the return for an aircraft with terrain included. The aircraft will be 1500 ft AGL like in the *IMOM* experiments. This may allow some comparison between the two programs.

The fifth experiment combines the third and fourth experiments to test the impact of turbines and clutter on a radar's probability of detection. Because of the small scenario size limitation, this experiment can't be expanded to include multiple turbines with an aircraft flying.

An optional experiment is to separate the wind turbine model into two parts; one containing the blades and hub, the other containing the tower and nacelle. Next, leverage *INSSITE's* ability to dynamically move objects to rotate the turbine blades in a realistic manner. This would enable the collection of phase data to generate a complete RCS analysis.

3.5.3 Underlying Mathematics. In each of the above experiments, the impact of sidelobe and backlobe interference must be included. Even though sidelobes may be 20 to 30 dB down from the mainbeam, turbines with a RCS of 30 to 40 dB can still interfere with the detection of small mainbeam targets. Figure 3.4 shows a range ring and several lobes. The length of the lobes is an indication of relative power.

For each cell the received power should be calculated using the radar range equation (2.1). Many of the terms in the equation are the same for every cell within a range ring and can therefore be rolled into a constant, C_i . That simplifies the equation for power received, $P_{r,i} = C_i G_i^2 \sigma_i$, for individual cells. The total received power at one instant,

$$P_r = \sum_{i=1}^N P_{r,i}, \quad (3.3)$$

accounts for the contributions from every lobe. The values of σ_i can come from terrain, aircraft, and turbines.

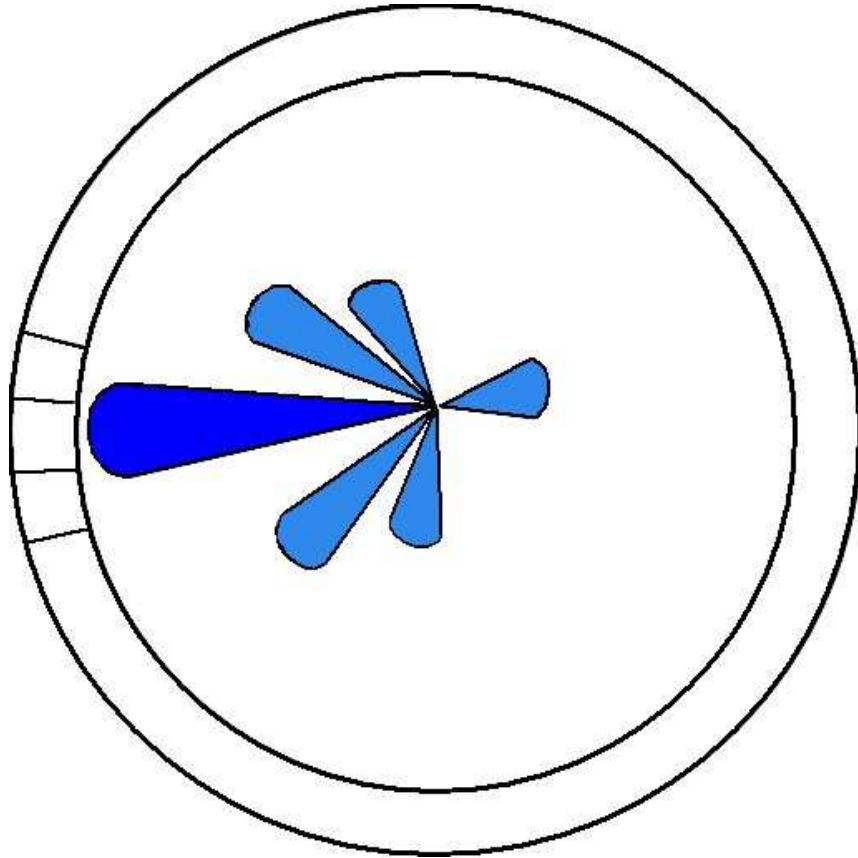


Figure 3.4: Range ring showing how sidelobes and backlobes contribute to the total received strength for a single range cell.

3.6 Analyzing the Architecture

The goal of this effort is to determine which areas of the architecture need further development. To accomplish the task, components of the proposed framework were compared with capabilities inherent to *IMOM* and *INSSITE*. If neither of the programs could perform one of the functions at the appropriate M&S level, then that function is tagged for further development. Whereas, components that are already at the correct M&S level should be leveraged rather than redesigned. This prioritizes the research areas requiring additional funding.

IV. Radar-based Modeling and Simulation

This chapter breaks the simulation into components and discusses the products and objectives at each level. First, the mission-level which provides the glue for all the components is highlighted, followed by a brief discussion of the connections between lower level components. Finally, the individual components are separated and evaluated for requirements at engagement, engineering, and physics-levels.

4.1 Connection Diagrams

This section will traverse the tiers of the M&S pyramid to show how the models will interact. When data is requested but isn't available, the model will push-down to a lower level to generate the data. For example, a radar requests a simple aircraft RCS, at the engagement-level, but that data isn't known. The aircraft RCS feature will drill down to the engineering level to find a suitable solution or to the physics level to generate the data. If it's not reasonable, cost or time prohibitive, to generate the data, an error message will notify the user.

4.1.1 Mission-Level. Figure 4.1 depicts the mission-level simulation where statistical objectives are generated from a large number, thousands or tens of thousands, of repetitions of the engagement-level M&S. At the highest level, the simulation should output data on how interactions between the radar, aircraft, clutter, and/or structures affect radar probability of detection [28]. In addition, some information/knowledge about the effect changing structures and/or locations has on radar performance should be generated [28]. The objective of the simulation is to determine radar performance measures for aircraft detection despite environmental interference, clutter and large moving structures like wind turbines [28].

Once the hypothesis tests are developed, the evaluation process can be automated to produce a radar coverage map. In addition, the analysis results must be conveyed in a straightforward manner. Figure 4.2 shows a simplistic FAA tool for determining if a turbine location might interfere with a radar [2]. The proposed radar

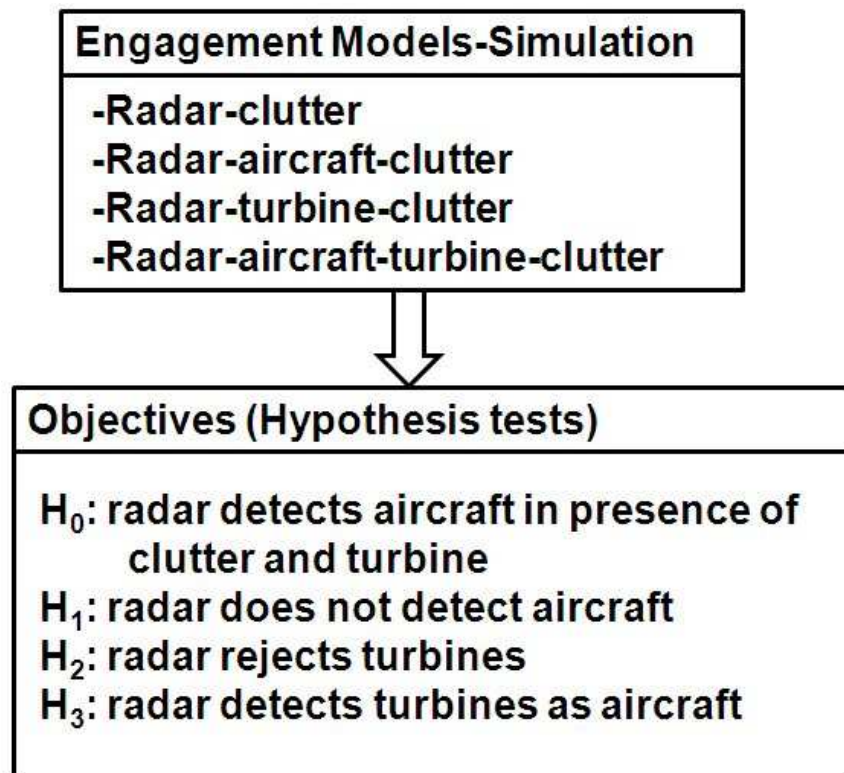


Figure 4.1: The mission-level simulation depends on lower-tier, engagement, simulations. The objectives are in the form of hypothesis tests [28].

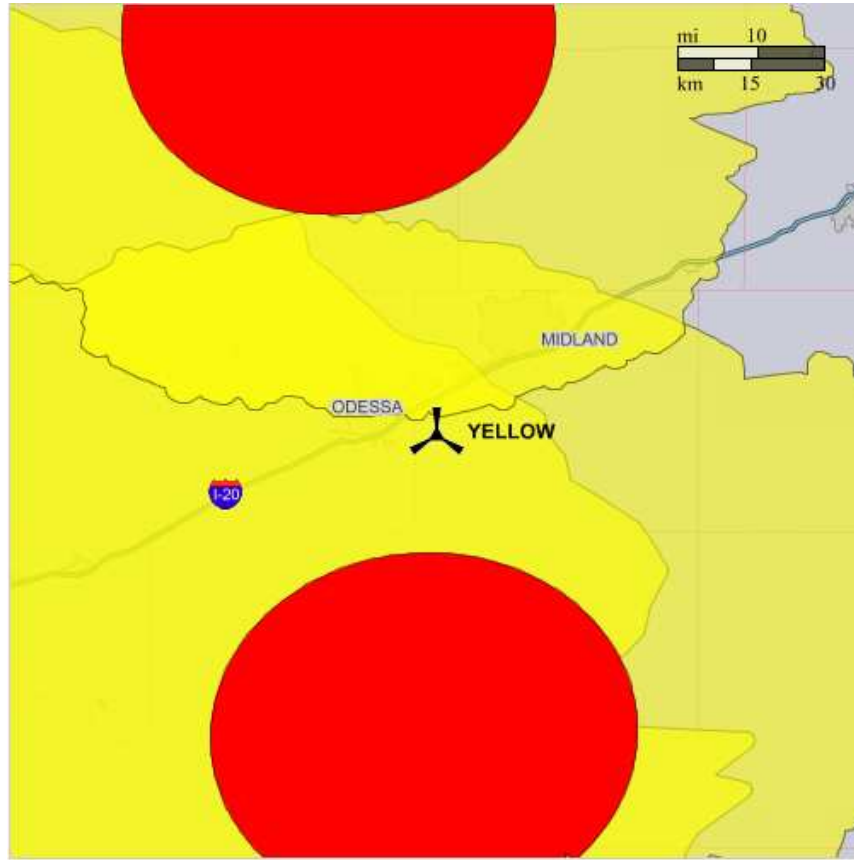


Figure 4.2: FAA tool, Obstruction Evaluation/Airport Airspace Analysis (OE/AAA), performs rough analysis to determine if a proposed wind turbine site requires additional analysis. The colored circles represent areas requiring additional analysis [2].

coverage map should look similar to Figure 4.2 but, it should provide analysis for each resolution range cell.

4.1.2 Engagement-Level. Figure 4.3 depicts the engagement-level simulation which is dependent on both engineering and physics-level M&S to generate the hypothesis tests [28]. The engineering-level models should be run many hundreds or thousands of times to account for changes in the receiver, processor, target RCS, and target Doppler. The hypothesis tests are derived by comparing the probability of detection between four scenarios: radar with clutter, radar with aircraft and clutter, radar with turbines and clutter, and radar with aircraft, turbines, and clutter.

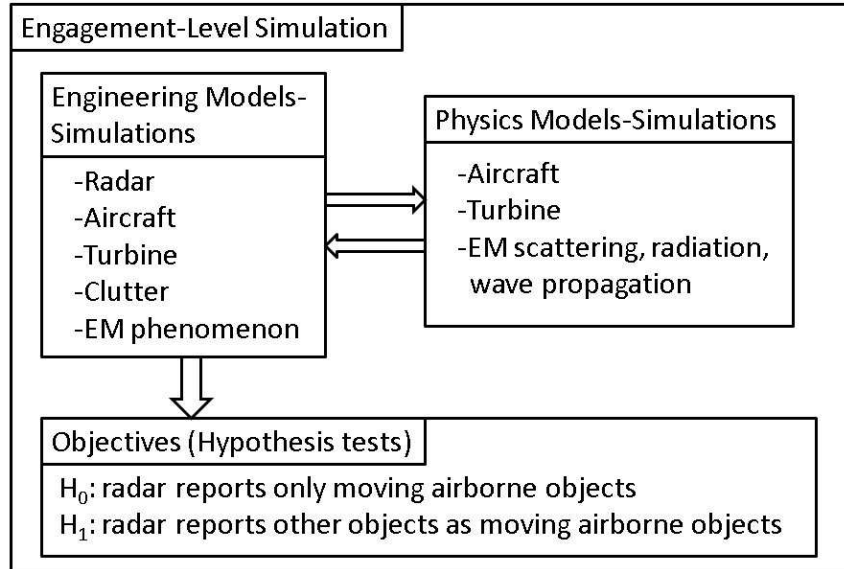


Figure 4.3: The engagement-level simulation depends on interaction between engineering-level M&S and physics-level M&S. The objectives are represented as hypothesis tests [28].

4.1.3 Engineering-Level.

4.1.3.1 *Radar.* The main component at the engineering-level is the radar model which is connected to the environment as presented in Figure 4.4 [28]. The radar itself has several subsystems, that are discussed later. The radar model follows the generic block diagram used in several text books [9] [30]. When modeling radars, the topic of signal-level versus parametric modeling is always at the forefront. Signal-level models represent pulse features, with nanosecond accuracy, for the time step of radar signals. Signal-level modeling is synonymous with physics-level modeling. Whereas, parametric models use pulse repetition interval, several milliseconds, for the time step and define the radar signal by a few parameters (amplitude, pulse width, frequency, and modulation) [28]. Because of the lower level of detail, parametric modeling is equivalent to engineering-level modeling. Signal-level models are the most detailed and accurate radar models.

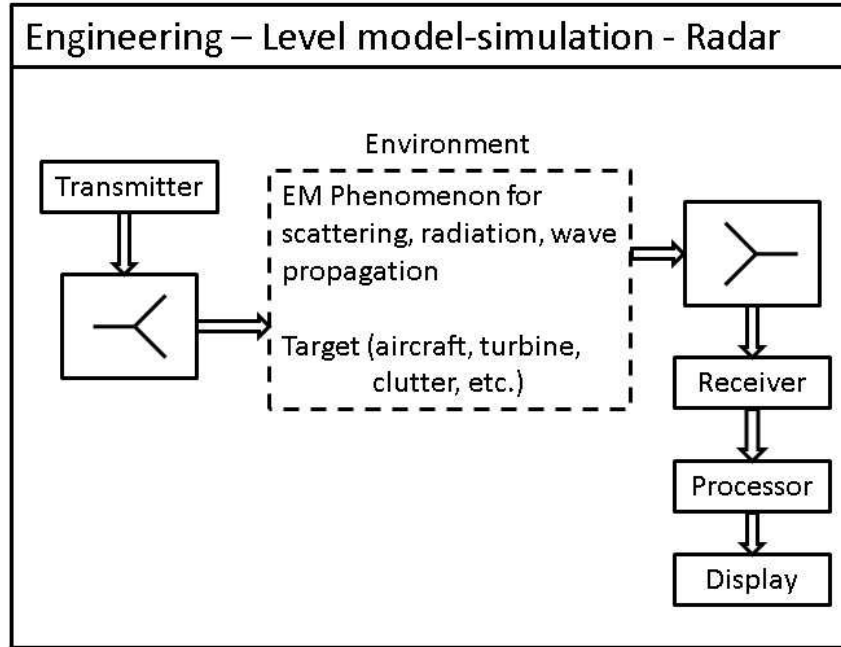


Figure 4.4: The main engineering-level model is the radar model, it connects the other engineering and physics models together through the environment component [28].

4.1.3.2 *Environment.* The environment block is key because it ties together the radar, electromagnetic (EM) phenomenon, and target engineering and physics models. The main difference between engineering-level and physics-level EM models are the density of the observation grid and the number of assumptions used. In addition, engineering-level EM models can use previously processed physics data, in the form of look-up tables and scattering centers for aircraft and turbine signatures [28].

The term “targets” encompasses aircraft, clutter, turbines, and other large structures. Clutter models are often statistical functions, based on a terrain scattering coefficient [9], that can be thought of as engineering-level models. The engineering-level model of the aircraft and turbine are characterized by scattering center models and/or look-up tables.

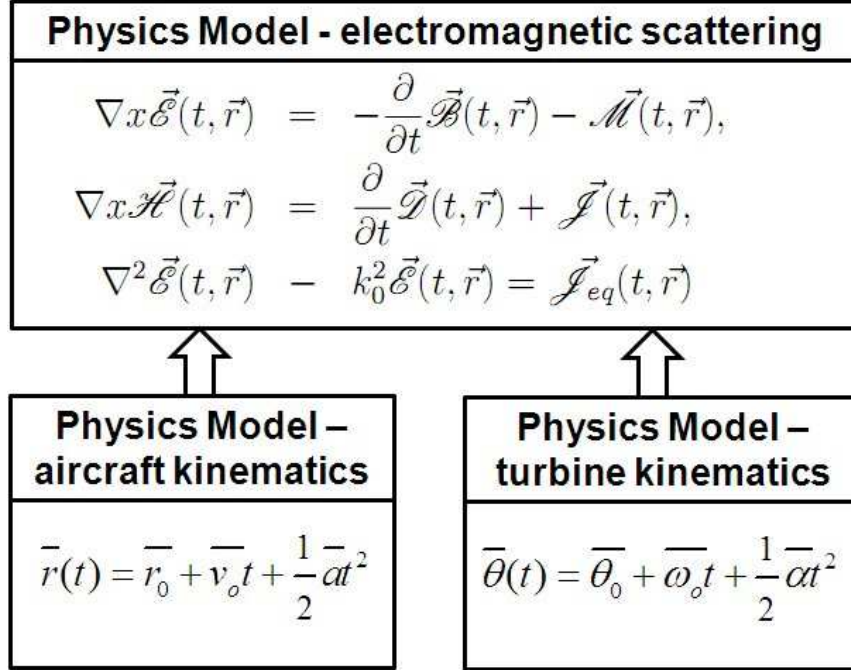


Figure 4.5: The physics-level M&S for EM wave scattering from a moving target. Maxwell’s equations form the basis of the EM physics model, but the simulation also requires a moving target model (aircraft or turbine) [28].

4.1.4 Physics-Level. Figure 4.5 depicts the highest fidelity physics model for EM wave scattering. Maxwell’s equations are solved for moving aircraft and turbines to determine the amount of scattered energy. Simulations at this level are very detailed and require intensive processing that should be avoided for typical analysis. This simulation level is required when pre-processed data isn’t available or when attempting to study basic effects such as the time-evolution of the scattered EM waves.

4.2 Features

This section defines several features or components in the context of the M&S architecture. The following list contains features that are discussed.

- Display
- Radar - Transmitter

- Radar - Antenna
- Radar - Receiver
- Radar - Signal Processor
- Target - Aircraft Motion
- Target - Turbine Motion
- Target - Clutter
- EM - Propagation

4.2.1 Display. At the mission-level, the display component would show a low resolution, much larger squares than range resolution cells, radar coverage map based on power levels. At the engagement-level, the display consists of a red/yellow/green stoplight map based on LOS, probability of detection, and false alarm. At the engineering-level, the display should operate like a PPI for one or multiple scans.

4.2.2 Radar. For simplicity, at the engagement-level many radar components are modeled as strict power gain or loss in dB. The objective is to calculate relative power received, $P_r \approx P_t + G_{tx} + G_{rx} + \sigma - L$. Parametric or engineering-level models are an expanded version of the radar range equation (2.1) [30]

$$R_{max}^4 = \frac{P_{av} G A \rho_a \sigma n E_i(n) F^4 e^{-2\alpha R_{max}}}{(4\pi)^2 k T_0 F_n(B\tau) f_p(S/N)_1 L_f L_s}. \quad (4.1)$$

Signal or physics-level models are the most accurate representation of a radar signal. The equations for the signal models are discussed under each component rather than assembling one large equation.

4.2.2.1 Transmitter. The transmitter is the component that generates the signal to interrogate the environment. The transmitter is described by many variables: bandwidth, power, pulse width, operating frequency, pulse repetition frequency, and waveform. A parametric model can incorporate all of those variables and

more. The definition of the transmitter output is

$$S(t) = \sum_{m=0}^{M-1} A_o a_o \left(\frac{t - mTp}{\tau} \right) \cos(2\pi f_o t + \theta_o), \quad (4.2)$$

for a rectangular pulsed signal.

4.2.2.2 Antenna. Antennas are the interface between a radar and the environment. Depending on the application, the transmit antenna may be different than the receive antenna. Antenna beams are characterized by several variables: gain, shape, azimuth and elevation beam widths, mismatch loss, sidelobe locations, frequency range, and scan rate. Parametric models will use a subset of those variables. The physics-level representation of the antenna

$$\alpha_t(t) = \sqrt{\frac{G(\theta(t), \phi(t))}{L_D L_C}}, \quad (4.3)$$

requires a continuous equations for gain, $G(\theta(t), \phi(t))$, duplexer loss, and coupler loss.

4.2.2.3 Receiver. The receiver is responsible for down-converting the radar returns to baseband or intermediate frequency and separating the signal into in-phase and quadrature components. The final part of the receiver is the matched filter. A parametric model of a receiver is characterized by its noise factor, dynamic range, bandwidth, and minimum detectable signal. In addition, a receiver may include pulse integration which is described by the number of pulses and integration efficiency. The signal-level model of the matched filter is

$$y_o(t) = \int_{-\infty}^{\infty} y_{in}(\lambda) s(\lambda - t) d\lambda. \quad (4.4)$$

4.2.2.4 Signal Processor. The processor designs, which vary from radar to radar, are pivotal to reducing wind farms impact on aircraft detection. Radar processors generally have several operating modes or channels which should be eval-

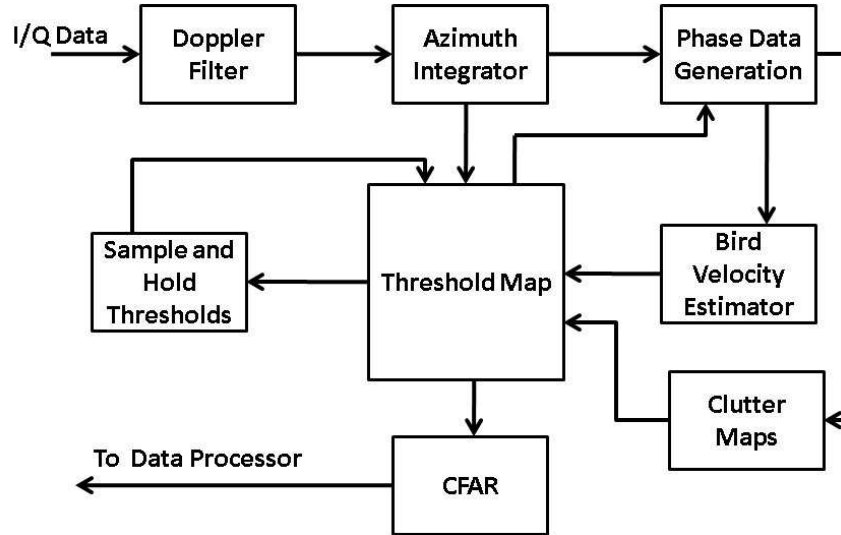


Figure 4.6: The processor of an ARSR-4 contains many filters which help determine detection thresholds [10].

uated individually and in conjunction to determine the optimal method for detecting an aircraft in the same or adjacent cell as complex clutter. Figure 4.6 presents the processor components within an ARSR-4 radar [10]. The individual blocks require physics-level detail to accurately model detections.

At the engagement-level the signal processor will have a detection threshold on top of any processing gains. The engineering-level will include the gain from it's algorithms along with the effects of clutter maps. The physics-level will have the actual algorithms to process signals.

4.2.3 Target. Targets include aircraft, turbines and clutter.

4.2.3.1 Aircraft Motion. Aircraft motion is important for Doppler processing and aircraft orientation is important for RCS measurements. Aircraft motion is simply range at the engagement-level. The engineering-level includes latitude, longitude, altitude, and velocity vector. The physics-level contains 6 degree of freedom along with velocity and acceleration vectors.

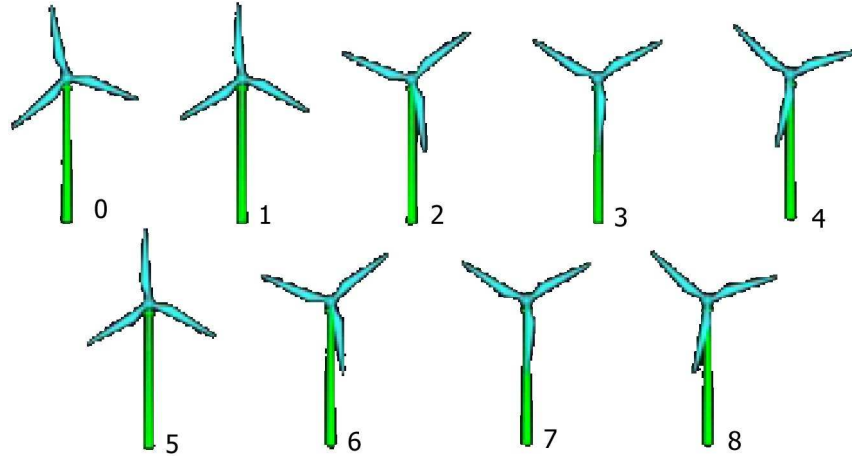


Figure 4.7: A discrete set of turbine blade positions used at the engineering-level [26].

4.2.3.2 Turbine Motion. Turbine motion, like aircraft motion, is important for Doppler processing and turbine positioning effects RCS measurements. Turbine motion at the engagement-level is merely the wind farm location. At the engineering-level, there is a discrete set of blade rotations along with turbine location, like in Figure 4.7 [26]. The physics-level model will include the continuous motion of the blades.

4.2.3.3 Clutter. Clutter is unwanted radar returns from terrain, foliage, and buildings. At an engagement-level, clutter is summarized as a negative RCS because it reduces the ability to detect an intended target. For the engineering-level, clutter is modeled as a distribution function [30]. The physics-level clutter model accounts for range dependent dielectric constants.

4.2.4 EM - Propagation. Wave propagation accounts for factors like atmospheric loss and terrain features to determine how far a signal can travel. Conditions like rain, fog and foliage will reduce the maximum detection range and produce clutter. At the engagement-level propagation is a straightforward attenuation factor. The engineering-level model includes some effects like diffraction, LOS, and multi-path due to ground or atmospheric ducting are included. Figure 4.8 illustrates a

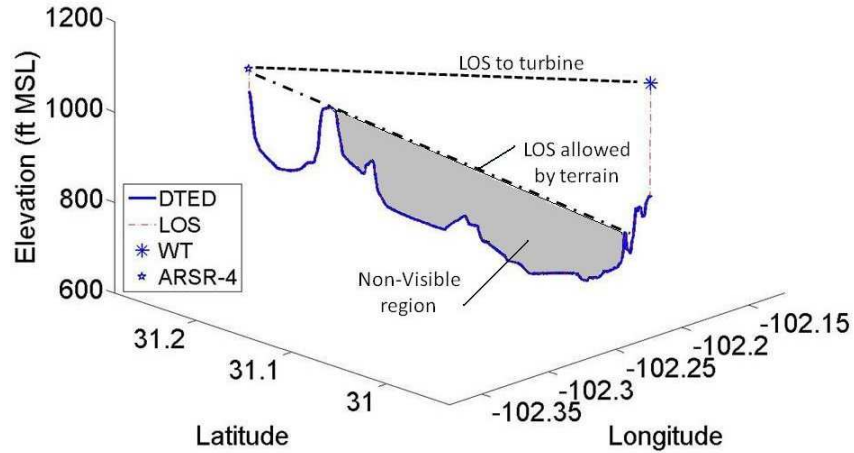


Figure 4.8: A slice of terrain evaluated for LOS [10].

Table 4.1: Sample radar and turbine parameters

Parameter	Symbol	Value
Wavelength	λ	0.25 m
Pulse Repetition Frequency	PRF	288 Hz
Azimuth Beamwidth	θ_B	1.5 deg
Radar Scan Rate	T_R	12 sec
Tower Height	h_t	80 m
Tower Diameter	d_t	3 m
Blade Length	l_b	40 m
Blade Rotation Rate	ω_b	2 rpm

LOS tool that accounts for $4/3^{rd}$ s earth radius and the first Fresnel zone [10]. A physics-level propagation model is a full parabolic equation that handles all of the possible engineering-level options. Figure 4.9 shows three different propagation models. APM and VTRPE are physics-level models while TIREM is an engineering-level propagation model.

4.3 Understanding Computational Requirements

The following example illustrates how expensive it is to calculate scattering centers for a wind turbine. The radar parameters are outlined first. Then, the turbine parameters are generated.

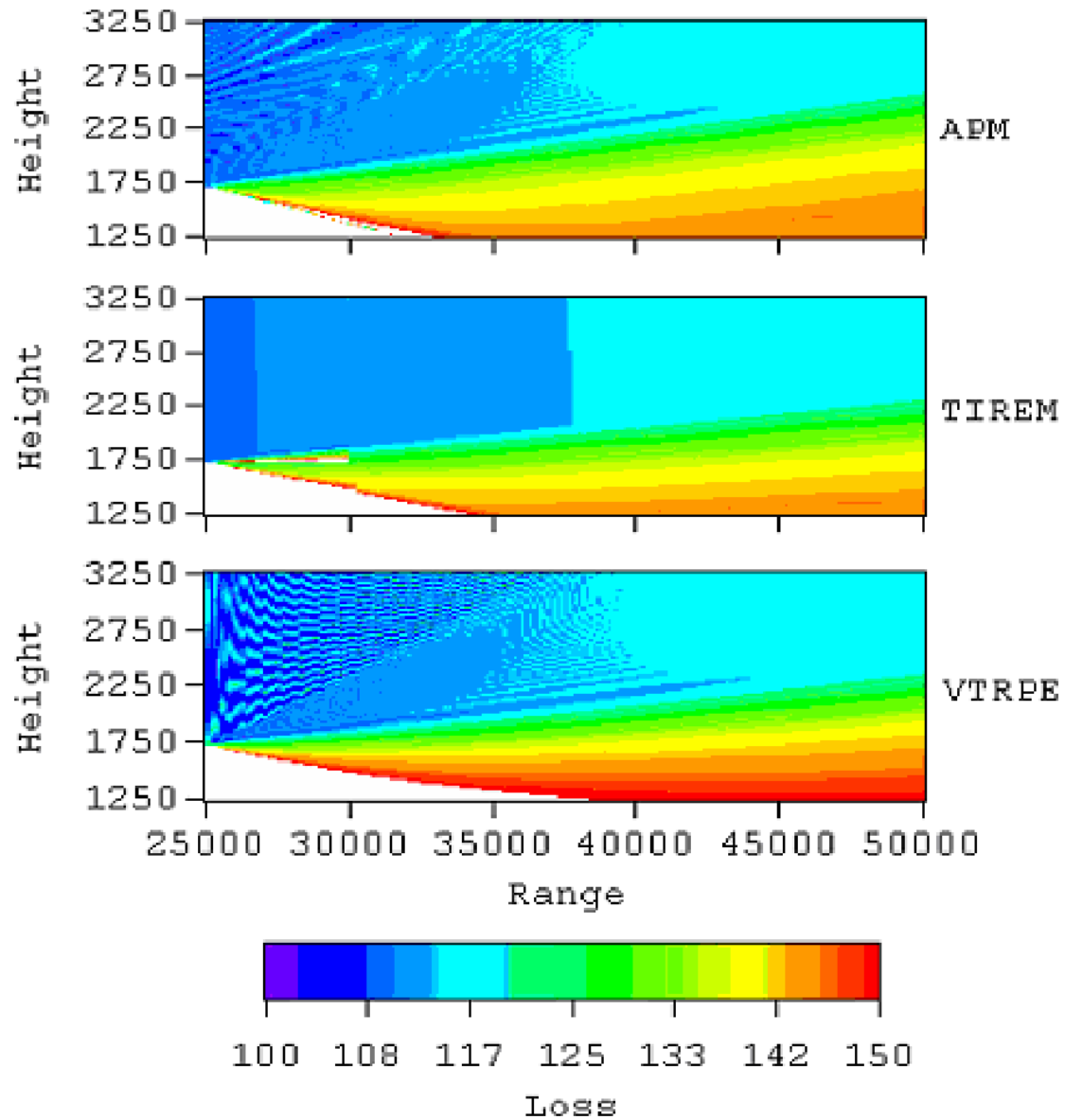


Figure 4.9: TIREM is an engineering-level propagation model whereas APM and VTRPE are physic-level models [27].

A quick example, using the parameters from Table 4.1, shows how many pulses hit a target in one sweep of a radar. The illumination time $t_i = T_R \theta_B / 360$ tells how long the beam illuminates a point target. The number of pulses per illumination is given by $N_p = t_i PRF$. For this example the number of pulses per illumination is 14.4, which is seemingly benign when considered independently. Next, the turbine RCS measurements are calculated to put the value into perspective.

This example estimates the required number of measurements for different blade positions. Following Nyquist, the required rotational sampling can be calculated by $\phi_s = (360/60)(\omega_b/PRF)/2$, or 0.21 deg. Turbine blades are usually radially symmetric, which reduces the required number of measurements for different blade positions to $N_{RCS} = 120/\phi_s$. Again, the number 576 seems benign on its own. However, that implies 576 RCS models need to be evaluated using (3.1) to generate a look-up table for one turbine, at one rotation rate. If physics-level RCS measurements are taken, then each run could take multiple hours.

Another method for modeling an object's total RCS

$$\sigma \approx \sum_{i=1}^N \sigma_i e^{-j \vec{k} \cdot \vec{r}_i}, \quad (4.5)$$

relies on a collection of i scattering centers [20]. The turbine blades can be modeled as a flat disc connected to a rectangle. The total surface area of the turbine $A = \pi l_b^2 + (h_t - l_b) d_t$ is approximately 5146 m². The Nyquist sampling area $A_s = (\lambda/2)^2$ is 1/64 m² for the radar. The maximum number of scattering centers $N_{sc} = A/A_s$ is approximately 330,000. These calculations are less complex and faster to compute than physics-level equations.

4.4 Rationale behind Tip Speed - Wind States

If two turbines have different length blades, 30 m and 50 m, but the same tip speed, the maximum Doppler shift would be the same for both turbines. However, if the same two turbines were rotating at the same rate, then the 50 m turbine would

Features	IMOM	INSSITE	Ideal
Transmitter	Y	Y/O	Y/O
Antenna	Y	Y/O	Y/O
Receiver	Y	Y/O	Y/O
Signal Processor	G	G/Y	Y/O
Display	B/G	Y/O	B/G/Y
AC Motion	G/Y/O	G/Y/O	G/Y/O
Turbine Motion	R	G/Y/O	G/Y/O
Clutter	Y/O	Y/O	G/Y/O
Doppler	R	O	G/Y/O
RCS	G/Y	Y/O	G/Y/O
Propagation	Y/O	O	Y/O

Mission (B)
Engagement (G)
Engineering (Y)
Physics (O)
None (R)

Figure 4.10: The physics-level M&S for EM wave scattering from a moving target. Maxwell's equations form the basis of the EM physics model, but the simulation also requires a moving target model (aircraft or turbine) [28].

have a higher maximum Doppler shift. In addition, if two turbines have the same length blades but different gearing ratios, the blades will turn at different rates given the same wind speed and again produce different Doppler shifts. Tip speed is the most consistent turbine measurement that relates to maximum Doppler shift. The one caveat is that relative wind direction has an impact on tip speed and Doppler as shown previously. Therefore, Table 2.4 will need to be expanded to include relative wind direction along one axis and tip speed along the other.

V. IMOM and INSSITE Experiments

This chapter discusses experiments using IMOM and two of SAIC’s in-house evaluation tools, *INSSITE* and *RF Scene*. The first step is to introduce the tools. Secondly, the results of the experiments are presented. Then, each program is dissected to compare their functions to the components of the M&S framework. Finally, their limitations for evaluating wind farms are highlighted.

5.1 IMOM

5.1.1 Overview. *IMOM* was developed to predict the effect of electronic support and electronic attack systems on “radar, weapon, communication and passive detection sites within an electronic order of battle (EOB)” [17]. At a basic level, *IMOM* evaluates parametric models for EW systems to determine when radars will detect an aircraft.

5.1.2 Experimental Results. The results of the four *IMOM* experiments are detailed in the following sections.

5.1.2.1 LOS. *IMOM* handles LOS detection based on a target altitude. There are two elevation modes: mean sea level (MSL) and above ground level (AGL). MSL is an absolute elevation which lends itself to aircraft positions. AGL is altitude relative to terrain which fits the analysis of turbines. Unless the terrain is perfectly flat the two elevation modes will create slightly different LOS results.

Once elevation is determined the actual LOS calculations can be performed. The LOS calculations are incorporated within propagation algorithms. The calculations are based on the actual earth radius or $4/3^{rd}$ radius approximation. The accuracy of each method is directly related to the resolution of the terrain data. In addition, some of the propagation models account for diffraction and Fresnel zones to improve accuracy. Figure 5.1 shows the LOS blockage around King Mountain, TX of a 0.001 m² target at 200 ft AGL using the terrain integrated rough earth model (TIREM) over level 1 DTED. The southwest area is mostly obscured at this elevation.

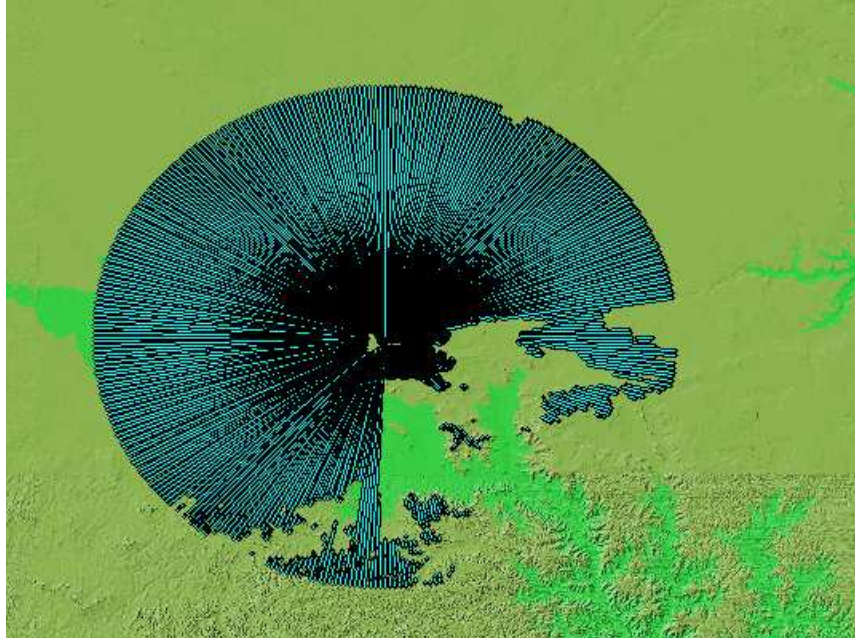


Figure 5.1: Depicts *IMOM*'s ability to account for terrain masking. The 0.001 m^2 calibration target was placed at 200 ft AGL.

5.1.2.2 Aircraft Detection. To explore radar-aircraft-terrain interactions, a low flying, 1500 ft AGL, aircraft with 1 m^2 RCS was evaluated. The low altitude was chosen to increase the effect of terrain interference. Figure 5.2 shows the results of the simulation. The limiting factor was still terrain masking. If the aircraft RCS was a factor there would be a circular pattern like in Figure 5.1.

5.1.2.3 Turbine Detection. This analysis is similar to the aircraft detection. LOS was detected for a much larger target, $10,000 \text{ m}^2$. The results in Figure 5.3 show the areas that a 200 ft tall turbine would be detected. These results can be used to tell contractors which areas are ideal, from the radar's perspective, for building wind turbines. However, these results don't provide details for the extent of impact on aircraft detection.

5.1.2.4 Aircraft-Turbine Interaction. The fourth experiment explores the possibility of modifying DTED by stitching a wind turbine into the file. Once

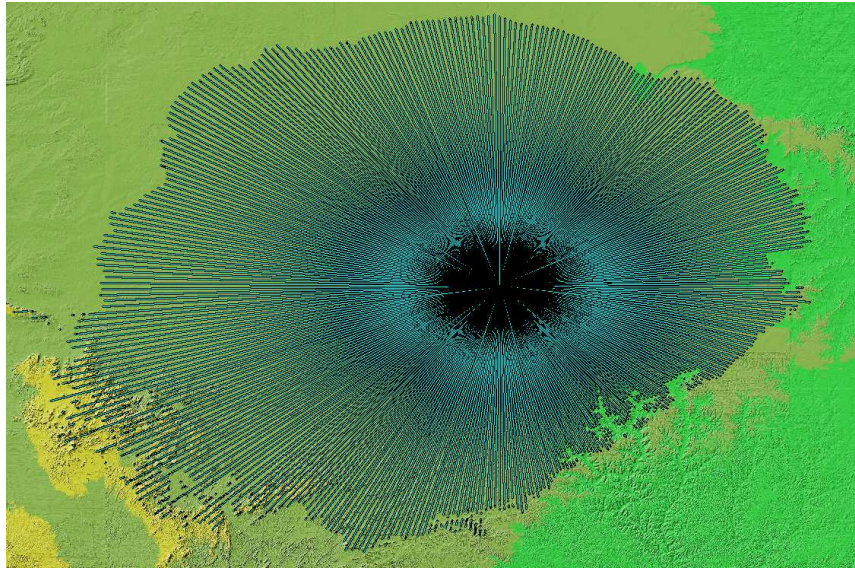


Figure 5.2: Depicts *IMOM*'s ability to detect an aircraft at 1500 ft AGL.

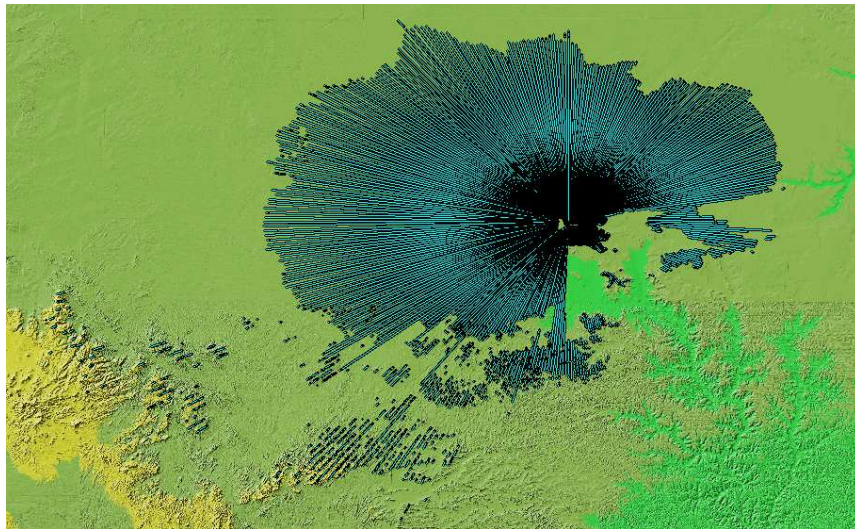


Figure 5.3: Depicts *IMOM*'s ability to detect a wind turbine at 200 ft AGL.

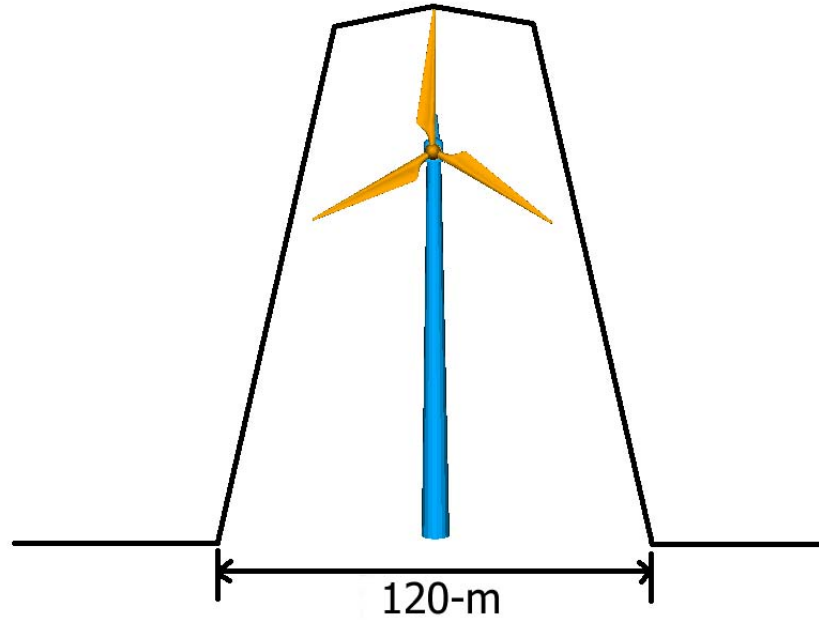


Figure 5.4: Modified level 2 DTED to account for wind turbine shadow zones.

the elevation data is adjusted, LOS calculations account for shadow zones. A first order approximation adjusts the height of specific key nodes to create a hill. Fig. 5.4 shows a worst case example of the affect of adjusting a couple key elevation nodes. Fig. 5.5 shows the best case example of using terrain to approximate shadow zones. As expected, DTED level 2 creates a smaller cross sectional area than DTED level 1 and a much smaller area then DTED level 0. The LOS analysis of shadow zones, using modified DTED level 2, should provide accurate results for a single turbine. When turbines are arranged in a wind farm, the best course of action could be to create an artificial plateau covering the whole farm. In that situation, the effect of DTED levels would decrease as the farm size increased. However, no physical DTED files were actually manipulated. An open-source program showed the potential to modify DTED [1].

The second part of the fourth experiment was the idea of modeling turbines as a radar jammer. If the turbine is modeled as a continuous noise jammer, it would reduce the radar detection range in all directions. A self-protection jammer that acts

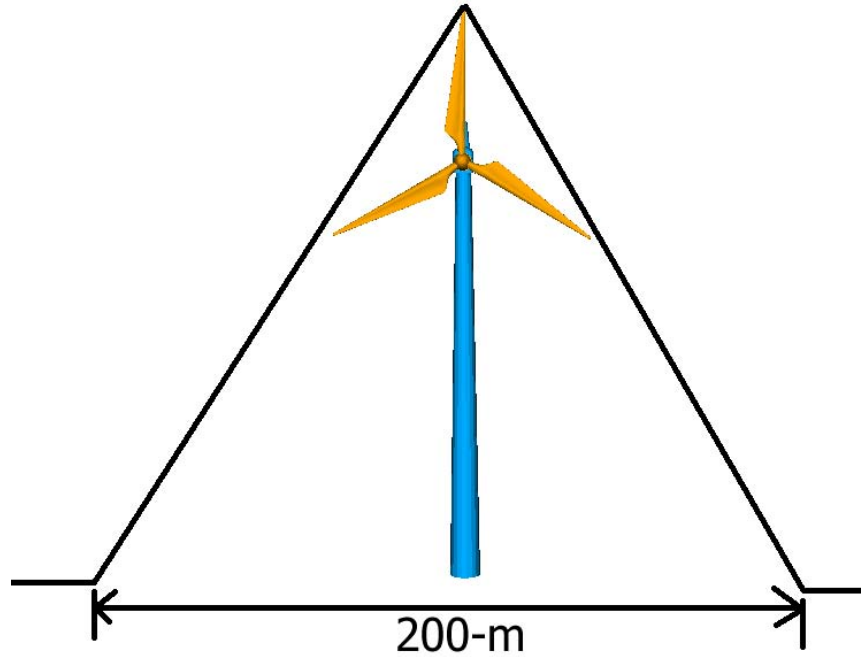


Figure 5.5: Modified level 1 DTED to account for wind turbine shadow zones.

as a repeater with large gain may be a reasonable approximation. Because of time constraints this portion was not investigated.

5.1.3 Mission-Level. *IMOM* is often used as a mission-level model by running Detection Contours or Detection Radials. The EOB can account for complete integrated air defense systems (IADS), EW strike packages, and EW support packages. The scope of some EOBs border on campaign-level.

5.1.4 Engagement-Level. When running a contour or radial analysis, area of interest and detection grid are specified. The analysis relies on several physics and engineering-level models: parametric radar, antenna patterns, propagation effects, aircraft route and RCS, and terrain masking. However, it cannot test whether moving ground structures are reported as moving aircraft.

5.1.5 Engineering-Level. Radar parametric and propagation models are two of the strengths of *IMOM*. The radar, antenna, and receiver subsystems were

adequately modeled to be considered engineering-level. Route planning is available which is an engineering-level version of target motion. The TIREM propagation model performed LOS, rough atmospheric loss, and clutter effects at an engineering-level. In addition, *IMOM* can process a 3D RCS pattern which is necessary for engineering-level analysis.

5.1.6 Physics-Level. Most components of *IMOM* operate above the physics-level. Propagation components are the exception. There are two very accurate models included with *IMOM*, variable terrain radio parabolic equation (VTRPE) and advanced propagation model (APM). APM is a hybrid model that uses different equations based on elevation and range. VTRPE is a full parabolic equation that provides the most accurate propagation model [27]. Both models include range dependent dielectric constants for measuring clutter.

5.1.7 Limitations.

- Parametric model doesn't provide I/Q data necessary for radar phase, Doppler shifts.
- Signal processor algorithms aren't included.
- Only one target can be evaluated at a time, meaning analysis of radar-aircraft-turbine interaction can't be done, unless the turbine is literally part of the clutter.

5.2 INNSITE

5.2.1 Overview. *INSSITE* is a 3-D environment builder that allows users to create or adjust terrain, incorporate features, like vegetation, and attach 3-D models of structures. The scenes developed in *INSSITE* are evaluated by other tools, like *RF Scene* or *X Scene*. One of the selling points is its simulation ability that allows developers to view their environment in motion, before running any time consuming evaluation tools.

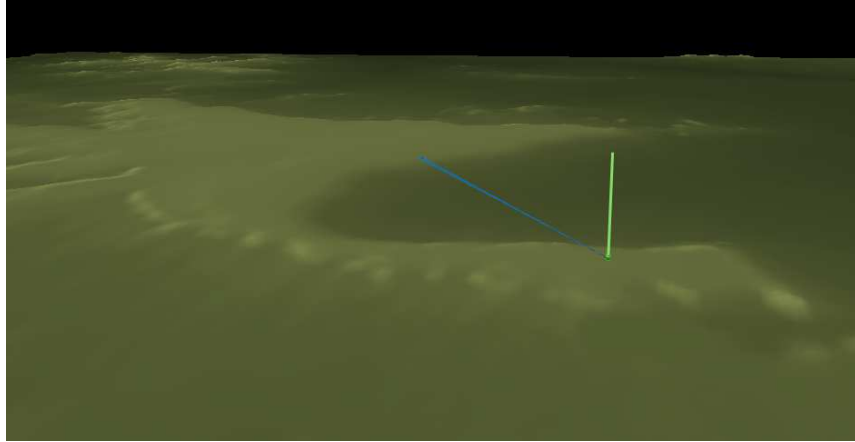


Figure 5.6: King Mountain, TX view from the north of the mesa.

RF Scene is an evaluation tool that operates on scenes created in *INSSITE*. *RF Scene* uses a shooting and bouncing ray (SBR) technique to analyze the RF spectrum for radar signals at the signal level. That means SBR provides amplitude and phase data for each ray. The addition of phase data enables the calculation of Doppler shift. SBR is covered in great depth in Knott [20], including the various diffraction methods available in *RF Scene*.

5.2.2 Experimental Results. Because of time constraints and technical difficulties using *RF Scene*, the experiments were setup but not evaluated. Figure 5.6 was a scenario with a radar illuminating hilly terrain. The experiment would have depicted the effect of clutter on a radar. Figure 5.7 shows the turbine and radar in freespace. Repeated analysis should be performed to determine the optimal observation grid for acceptable simulation accuracy and time. Figure 5.8 combines the previous two experiments to include the added effect of multi-bounce. Figure 5.9 mimics the *IMOM* test showing radar-aircraft-clutter interactions. Figure 5.10 would have been the capstone experiment showcasing the effect of turbines on probability of detection.

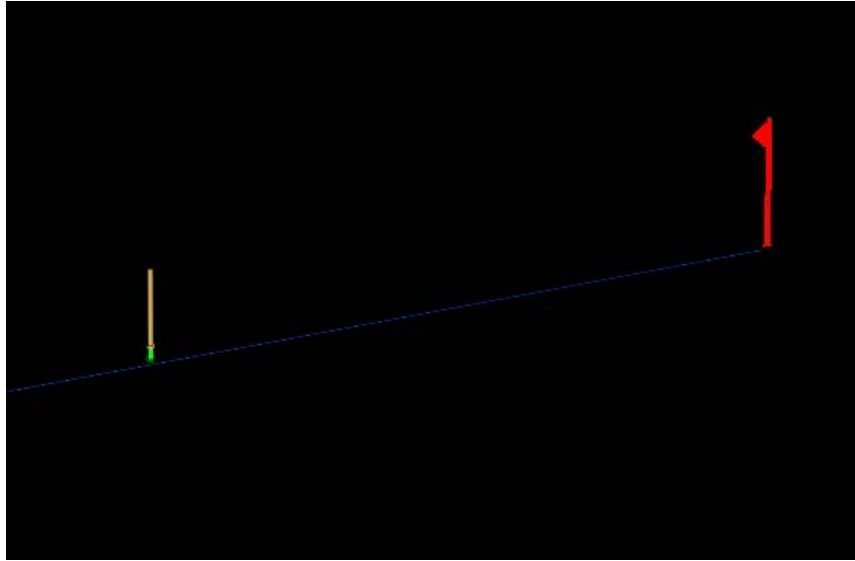


Figure 5.7: Measurements of a turbine in freespace to determine the most efficient observation grid.

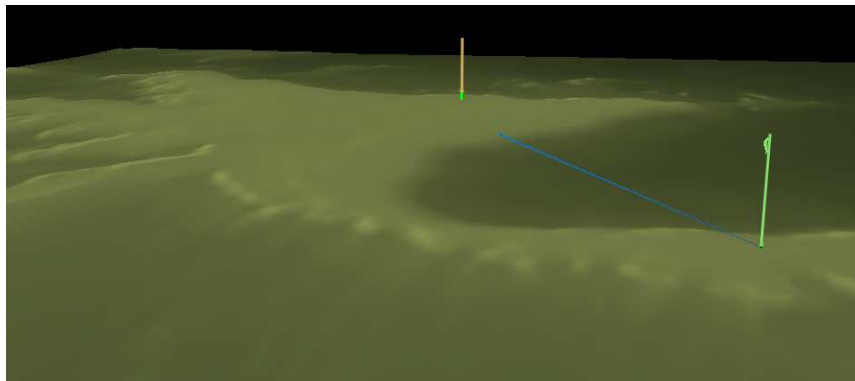


Figure 5.8: Scenario designed to measure the clutter environment to include a turbine.

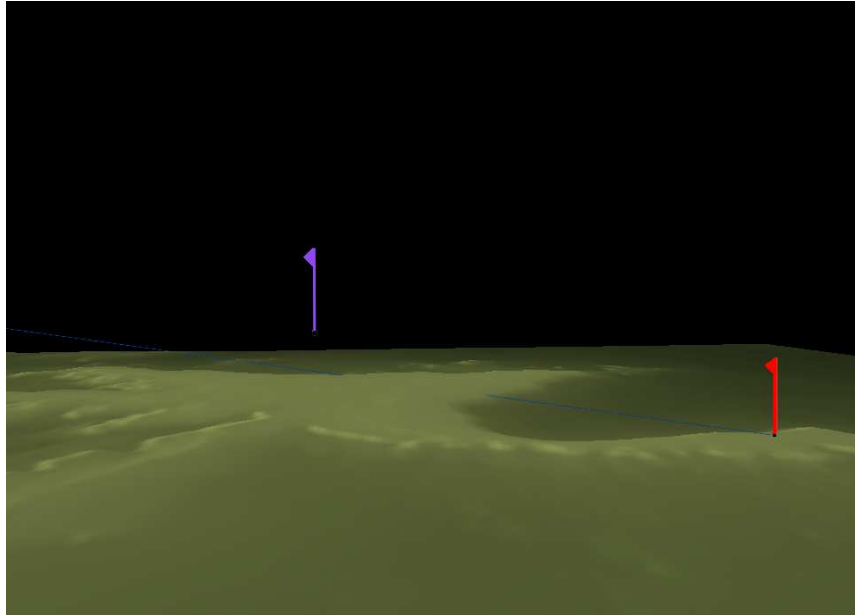


Figure 5.9: Scenario involving an aircraft 1500 ft above the mesa.

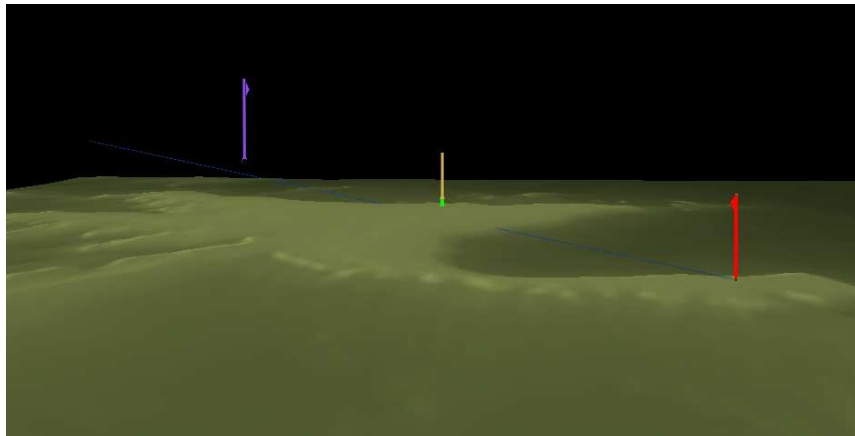


Figure 5.10: The ideal test scenario, includes radar, aircraft, turbine and terrain.

5.2.3 Mission-Level. *INSSITE* is capable of setting up a scenario that includes multiple objects and sensors. However, simulating a large scene, like a full farm, could take several days to process.

5.2.4 Engagement-Level. Engagement-level is where *INSSITE* is best suited, smaller scenarios where moving objects are visible. It should be capable of analyzing radar-aircraft-turbine-clutter interactions including Doppler effects.

5.2.5 Engineering-Level. The radar model is simplistic and adequate. The radar is not as customizable as *IMOM*'s radar models, yet it provides the essential capabilities to produce the requested analysis. *RF Scene* allows the capture of phase, RCS, and clutter data at the engineering-level. There are also hooks to call *X-scene* for engineering-level RCS data. Targets in *INSSITE* can be manipulated to various degrees to include routes for aircraft, turbine blade positions and turbine direction.

5.2.6 Physics-Level. Target models and antenna patterns can be extremely well detailed in *INSSITE*. In addition, when *RF Scene* is run with a tight enough grid it can produce physics-level phase information. *X-Patch* is called for physics-level RCS analysis.

5.2.7 Limitations.

- Elevation angles are not accurate when approaching 0 deg from the horizon. Elevation angles above the horizon are impossible.
- Requires small scene sizes, approximately one range resolution cell, to evaluate within an hour.
- Hidden limit of 2^{31} rays, affects maximum scene size and ray density.
- Creating a functioning ground radar is tedious.
- No native tool for creating or modifying antenna patterns.

- No native tool can display results of *RF Scene*. SAIC did provide separate Matlab[®] code for this purpose.
- Program stability is an issue.

VI. Conclusions

This chapter discusses areas for further research and summarizes this research effort.

6.1 Conclusions

The proposed large-scale modeling and simulation approach will provide a framework for the development of a program to evaluate radar-aircraft-wind farm-clutter interactions. The ability to select different levels of simulation provides a modular, scalable analysis tool.

Many of the subcomponents are already developed and in use. Several of the blocks: EM scattering phase and magnitude data, radar models, propagation equations, target movement and terrain data are currently generated at the necessary engineering and physics levels. However, several components still need to be developed.

Transforming engineering and physics-level scattering data into engagement-level stochastic scattering information will reduce the complexity of the simulation. In addition, it will facilitate the analysis of full wind farms rather than single turbines. Since a subsection of the scattering data is transformed into information, the amount of physics-level data generated for each turbine is reduced.

Customizable signal processor algorithms and their ordering should be implemented. The effects of clutter cell sizes on detection thresholds should be included. Algorithms like MTI that reduce the impact of turbines must be included.

The effort to coordinate all the models and simulations across different M&S tiers is significant. The tool will need to analyze the interference and summarize it with a display.

Finally, there is a large amount of data that must be generated for this or any other solution to work. There should be a method to categorize wind turbines into a discrete number of classes to reduce the data requirements.

6.2 *Additional Research*

There are many opportunities to expand the efforts that were started for this research. *RLSTAP* is another radar program that operates between the physics and engineering-levels to provide RCS phase and magnitude measurements. It may provide additional validity to the hybrid large-scale modeling and simulation framework.

INSSITE has several components that should be studied further. Providing analysis of a rotating turbine blade is quite powerful. However, the first step is to get *RF Scene* running.

IMOM may be capable of simulating turbine interference through non-traditional methods. Manipulating the different jammer models could simulate turbine clutter to produce first order results quickly. The other option is to adjust the elevation of the terrain data which will at least show the shadow zone effect and part of the RCS interference.

Signal processor algorithms warrant further investigation. MTI techniques reduce the magnitude of turbine returns, there should be additional techniques to reduce the Doppler return. There needs to be a large set of doppler data to test the algorithms.

Finally, the study of wind states as a method of classifying turbine clutter merits deeper research. It may be capable of supplying the stochastic data missing from the proposed M&S architecture. Providing a quick look analysis would be very useful.

Bibliography

1. “Geospatial Data Abstraction Library”. <http://www.gdal.org>.
2. “Obstruction Evaluation/Airport Airspace Analysis”. <https://oeaaa.faa.gov>.
3. 84 RADES. <http://www.rades.hill.af.mil>.
4. Air Force Research Laboratory. *The Air Force Research Laboratory (AFRL) Mobile Diagnostics Laboratory (MDL) Wind Farm Turbine Measurements Fenner*, NY. Final report, July 20 2006.
5. AIR WARFARE CENTRE RAF LINCOLN (UNITED KINGDOM). *The Effects of Wind Turbine Farms on Air Defence Radars*. Technical Report AD Number: ADA466350, January 2005.
6. AIR WARFARE CENTRE RAF LINCOLN (UNITED KINGDOM). *The Effects of Wind Turbine Farms on ATC Radar*. Technical Report AD Number: ADA467441, May 2005.
7. AIR WARFARE CENTRE RAF LINCOLN (UNITED KINGDOM). *Further Evidence of the Effects of Wind Turbine Farms on AD Radars*. Technical Report AD Number: ADA466373, August 2005.
8. Amato, N.A., P.M. Brand, M.A. Saville, and M.J. Mendenhall. “Modeling Clutter from Windmill Energy Farms”. Air Force Institute of Technology, 2009.
9. Barton, D.K. *Modern Radar Systems Analysis*. Artech House, Inc., 1988.
10. Brand, P.M. *Modeling of Wind Turbine Doppler Effects on Primary Search Radar*. Ph.D. thesis, Air Force Institute of Technology, 2950 Hobson Way, Wright-Patterson AFB, OH, 45433, USA, 2009.
11. Brenner, M. and et al. *Wind Farms and Radar*. Technical Report JSR-08-125, MITRE Corporation, January 2008.
12. Butler, G. “Advanced Digital Tracker - Update”, May 2007. <http://www.all-energy.co.uk/UserFiles/File/2007GeoffButler.pdf>.
13. European Organisation for the safety of Air Navigation. “Assessment Methodology to Determine the Impact of Wind Turbines on ATC Surveillance Systems”, March 2008.
14. European Organisation for the safety of Air Navigation. “Wind Farm Impact Assessment Techniques and Mitigation Measures”, March 2008.
15. 453rd EWS. <http://www.afioc.afisr.af.smil.mil/offices/318/453/453ews/453.cfm>.
16. Halliday, D. *Fundamentals of Physics Extended*. Wiley and Sons, 8th edition, 2008. ISBN 978-0-471-75801-3.

17. Idaho National Laboratory. *Improved-Many-On-Many (IMOM) Engineer Help*. 453rd EWS, Lackland AFB.
18. Jamshidi, M. *Large-scale systems: modeling, control, and fuzzy logic*. 1997.
19. Kent, B.M. and et al. “Dynamic Radar Cross Section and Radar Doppler Measurements of Commercial General Electric Windmill Power Turbines Part 1: Predicted and Measured Radar Signatures”. *IEEE Antennas and Propagation Magazine*, Vol. 50(No. 2):211–219, April 2008.
20. Knott, E.F. and et al. *Radar Cross Section*. SciTech Pub., 2nd edition edition, 2004.
21. Lemmon, J.J. and et al. *Assessment of the Effects of Wind Turbines on Air Traffic Control Radars*. Technical Report NTIA TR: TR-08-454, National Telecommunications and Information Administration, July 2008.
22. Mahmoud, M.S. *Multilevel systems control and applications: A survey*. 1977.
23. Marshall, B.K. <http://www.geograph.org.uk/photo/667522>.
24. NASIC. <http://www.naic.wrightpatterson.af.smil.mil/TableView/mission.html>.
25. Office of the Director of Defense Research and Engineering. *Effect of Windmill Farms on Military Readiness 2006*. Technical report, Congressional Defense Committees, 2006.
26. QinetiQ Ltd. *Wind Farms Impact on Radar Aviation Interests*. Technical Report Report W/14/00614/00/REP, September 2003.
27. REMCOM. *ElectroMagnetic Propagation Integrated Resource Environment (EMPIRE) Basic Guide to RF Propagation Models*. 453rd EWS, Lackland AFB, 2007.
28. Saville, M.A. “Notes on Large Scale Modeling and Simulation”, Feb 2009.
29. Simpson, J. and E. Weiner. “Oxford English Dictionary”, 1989.
30. Skolnik, Merrill I. *Introduction to Radar Systems*. McGraw-Hill, Inc., 1221 Avenue of the Americas, New York, NY 10020, third edition, 2001. ISBN: 0072909803.
31. Theil, A. and L.J. van Ewijk. “Radar Performance Degradation due to the Presence of Wind Turbines”. *IEEE*, 6, 2007.
32. US Army. *Commander’s Appreciation and Campaign Design*. Technical Report Pamphlet 525-5-500, 2008.
33. U.S. Department of Energy. *20% Wind Energy by 2030*. Technical report, July 2008.
34. Vestas Wind Systems A/S. “V82-1.65 MW Brochure”. <http://www.vestas.com/en/wind-power-solutions/wind-turbines/1.65-mw.aspx>.
35. Wikipedia. <http://en.wikipedia.org>.

36. Wisner, R. and M. Bolinger. *Annual Report on U.S. Wind Power Installation, Cost, and Performance Trends: 2007*. Technical Report DOE/GO-102008-2590, U.S. Department of Energy, May 2008.

REPORT DOCUMENTATION PAGE

Form Approved
OMB No. 0704-0188

The public reporting burden for this collection of information is estimated to average 1 hour per response, including the time for reviewing instructions, searching existing data sources, gathering and maintaining the data needed, and completing and reviewing the collection of information. Send comments regarding this burden estimate or any other aspect of this collection of information, including suggestions for reducing this burden to Department of Defense, Washington Headquarters Services, Directorate for Information Operations and Reports (0704-0188), 1215 Jefferson Davis Highway, Suite 1204, Arlington, VA 22202-4302. Respondents should be aware that notwithstanding any other provision of law, no person shall be subject to any penalty for failing to comply with a collection of information if it does not display a currently valid OMB control number. **PLEASE DO NOT RETURN YOUR FORM TO THE ABOVE ADDRESS.**

1. REPORT DATE (DD-MM-YYYY) 26-03-2009	2. REPORT TYPE Master's Thesis	3. DATES COVERED (From — To) Sept 2007 — Mar 2009
--	--	---

4. TITLE AND SUBTITLE Modeling and Simulation Architecture for Studying Doppler-Based Radar with Complex Environments	5a. CONTRACT NUMBER DACA99-99-C-9999
	5b. GRANT NUMBER
	5c. PROGRAM ELEMENT NUMBER

6. AUTHOR(S) Nicholas J. Amato, Capt, USAF	5d. PROJECT NUMBER N/A
	5e. TASK NUMBER
	5f. WORK UNIT NUMBER

7. PERFORMING ORGANIZATION NAME(S) AND ADDRESS(ES) Air Force Institute of Technology Graduate School of Engineering and Management (AFIT/EN) 2950 Hobson Way WPAFB OH 45433-7765	8. PERFORMING ORGANIZATION REPORT NUMBER AFIT/GE/ENG/09-02
---	--

9. SPONSORING / MONITORING AGENCY NAME(S) AND ADDRESS(ES) 84 Radar Evaluation Squadron (Shawn Jordan) 7976 Aspen Avenue Hill AFB, UT 84056-5846 ((801)777-3290, shawn.jordan@hill.af.mil)	10. SPONSOR/MONITOR'S ACRONYM(S) 84 RADES/SC
	11. SPONSOR/MONITOR'S REPORT NUMBER(S)

12. DISTRIBUTION / AVAILABILITY STATEMENT
Approval for public release; distribution is unlimited.

13. SUPPLEMENTARY NOTES

14. ABSTRACT
This research effort develops a hybrid large-scale modeling and simulation framework that defines the requirements for a program to evaluate radar-aircraft-turbine-clutter interactions. Wind turbines and other moving structures can interfere with a radar's ability to detect moving aircraft because radar returns from turbines are comparable to those from slow flying aircraft. This interference can lead to aircraft collisions or crashes, reducing the safety for air traffic. Two radar applications, *INSSITE* and *IMOM*, were investigated to determine which of the subsystems, in the proposed architecture, are currently available and which need additional development. Current radar applications either delve too deep into details, requiring years to process, or too shallow, ignoring the Doppler effect and assuming a static scattering value. Engineering-level radar, radiation, propagation, and scattering models are already developed. However, engagement-level stochastic scattering, amplitude and phase, data aren't available. The hybrid modeling and simulation architecture could be realized once stochastic RCS models are developed.

15. SUBJECT TERMS
Wind turbine; large-scale modeling and simulation; pulse Doppler radar; radar cross section; line-of-sight

16. SECURITY CLASSIFICATION OF:			17. LIMITATION OF ABSTRACT	18. NUMBER OF PAGES	19a. NAME OF RESPONSIBLE PERSON	
a. REPORT	b. ABSTRACT	c. THIS PAGE			Maj Michael Saville	
U	U	U	UU	63	19b. TELEPHONE NUMBER (include area code) (937) 255-3636, ext 4719; michael.saville@afit.edu	